Space-fractional advection-dispersion equations with variable parameters: Diverse formulas, numerical solutions, and application to the Macrodispersion Experiment site data

Yong Zhang,[1] David A. Benson,[1] Mark M. Meerschaert,[2] and Eric M. LaBolle[3]

[1]   To model the observed local variation of transport speed, an extension of the homogeneous space-fractional advection-dispersion equation (fADE) to more general cases with space-dependent coefficients (drift velocity V and dispersion coefficient D) has been suggested. To provide a rigorous evaluation of this extension, we explore the underlying physical meanings of two proposed, and one other possible form, of the fADE by using the generalized mass balance law proposed by Meerschaert et al. (2006). When the classical Fick's law is replaced by its generalized form in the first-order mass conversation law, the original fADE with constant parameters extends to the advection-dispersion equation (ADE) with fractional flux (denoted as FF-ADE). When the net inflow of dispersive flux is from nonlocal concentration gradients following a fractional divergence, we get the ADE with fractional divergence (FD-ADE). When the total net inflow from both nonlocal advection and nonlocal concentration gradients follows a fractional form, the fADE contains fully fractional divergence (FFD-ADE). These three fADEs with constant parameters can also be obtained by proper choice of the two memory kernels in the nonlocal dispersive constitutive theory proposed by Cushman et al. (1994), while the space-variable fADEs correspond to the conditional nonlocal theory proposed by Neuman (1993) after specifying the general (Lévy-type) functional form of the random distribution. The corresponding Langevin Markov models can be found in many cases, where the Lagrangian stochastic processes can be conditioned directly on local aquifer properties at any practical, measurable level and resolution. The resulting Lagrangian random-walk particle tracking methods, along with previous numerical solutions using implicit Euler finite differences, distinguish and elucidate the plume behavior described by these fADEs. The fractional models are applied to fit the tritium plumes measured at the Macrodispersion Experiment test site. When the local parameters gleaned from the hydraulic conductivity (K) distribution are varied even slightly (i.e., a two-zone model), allowing the use of observed hydraulic conditions at the site, the model fits are well within the variability of the data. The extended fADEs describe the fast and space-dependent leading edges of measured plumes in the regional-scale alluvial system, which was underestimated and could not be fully captured by the original fADE with constant parameters. Applications also favor the FD-ADE model because of the ease of implementation and consistency with previous analysis of the K statistics.

Citation: Zhang, Y., D. A. Benson, M. M. Meerschaert, and E. M. LaBolle (2007), Space-fractional advection-dispersion equations with variable parameters: Diverse formulas, numerical solutions, and application to the Macrodispersion Experiment site data, *Water Resour. Res.*, *43*, W05439, doi:10.1029/2006WR004912.

1. Introduction

[2] Non-Fickian transport of conservative solutes frequently is observed in regional- or laboratory-scale flow fields that are nonuniform on multiple scales [e.g., *Levy and Berkowitz*, 2003; *Bromly and Hinz*, 2004; among many others; K.A. Klise et al., Comparison of laboratory−scale solute transport visualization experiments with numerical simulation using cross-bedded sand stone, *Water Resour. Res.*, in review, 2007]. Numerous numerical experiments indicate that the anomalous dispersion cannot be captured by the traditional second-order advection-dispersion equation (ADE) without detailed, decimeter-scale, information of the connectivity of high and low hydraulic conductivity (K) sediments [e.g., *Zheng and Gorelick*, 2003]. The spatially fractional-order

---

[1]Department of Geology and Geological Engineering, Colorado School of Mines, Golden, Colorado, USA.
[2]Department of Statistics and Probability, Michigan State University, East Lansing, Michigan, USA.
[3]Hydrologic Sciences, University of California, Davis, California, USA.

advection-dispersion equation (fADE) is one analytic technique that accounts for this kind of medium nonlocality and simultaneously accounts for convergence of a stochastic solute particle motion process to a limit distribution. The spatial fADE may broaden the applicability of the second-order ADE by describing the superdiffusive rapid transport, including heavy leading plume edges and faster-than-Fickian growth rates [*Benson et al.*, 2000a, 2000b, 2001]. Additional theoretical formulations can also account for the trapping of solutes in relatively immobile facies and are described later in this paper. The one-dimensional fADE with constant transport parameters is of the form [*Benson*, 1998; *Meerschaert et al.*, 1999]:

$$\frac{\partial C}{\partial t} = -V\frac{\partial C}{\partial x} + D\frac{\partial^{\alpha} C}{\partial x^{\alpha}}, \qquad (1)$$

where $C(x,t)$ is the aqueous concentration, V is the drift velocity, D describes the spread of the process, and α ($1 < \alpha \leq 2$) is the scale index indicating the order of fractional differentiation. When $\alpha = 2$, equation (1) reduces to the second-order ADE with constant parameters. The nonlocal fADE (1) has been used to simulate solute transport through unsaturated soils [*Pachepsky et al.*, 2001; *Zhang et al.*, 2005], saturated porous media [*Zhou and Selim*, 2003; *Chang et al.*, 2005; *Huang et al.*, 2006], streams and rivers [*Deng et al.*, 2004; *Zhang et al.*, 2005; *Kim and Kavvas*, 2006], and overland flow [*Deng et al.*, 2006].

[3] One purported reason to favor the fADE (1) is its parsimony: The correct choice of the scaling parameter α for a highly heterogeneous aquifer should rid D of the scale dependence inherited by assuming $\alpha = 2$. The scale effects are reflected by the order of the space fractional derivative α, which should remain relatively constant for a given medium. The dispersion coefficient D needs to be found for only one scale, and this can be done either by analyzing the statistics of the K field or by calibration. Earlier applications [*Benson et al.*, 2000a, 2000b, 2001; *Pachepsky et al.*, 2001] confirm this by demonstrating that a fADE with a mean groundwater velocity V and a calibrated, scale-independent, and constant dispersion coefficient D can fit or predict the measured plumes in heterogeneous material. On the other hand, the heterogeneity that gives rise to fractional-order transport can certainly be nonstationary, so the parameters might be functions of space (but perhaps not depend on plume scale). Recent applications show some of this possible discrepancy. *Deng et al.* [2004] found that the best fit scale index fluctuates irregularly with transport distance, and *Huang et al.* [2006] found that the best fit dispersion coefficient increases with scale. However, whether these findings prove the space dependency of parameters is debatable because they applied the space fractional ADE (1) to fit directly a solute retention process. However, possible space dependence of the fADE parameters has drawn attention recently, and we discuss *Huang et al.*'s [2006] fADE with space-dependent parameters below. *Lu et al.* [2002] extended *Benson et al.*'s [2001] one-dimensional fADE model of the Macrodispersion Experiment (MADE) site tritium plume to three dimensions. Their model was not calibrated, did not model fractional transport in the transverse direction, and did not account for transfer of mass to a relatively immobile phase. However, they found that the fADE with uncalibrated, constant parameters underestimates the measured distal plumes, and thus they

suggested a fADE with variable parameters to capture the irregular resident concentration distributions observed at the MADE site. *Huang et al.* [2006] proposed, and *Lu et al.* [2002] suggested intuitively, a new fADE

$$\frac{\partial C}{\partial t} = -\frac{\partial}{\partial x}[V(x)C] + \frac{\partial}{\partial x}\left[D(x)\frac{\partial^{\alpha-1} C}{\partial x^{\alpha-1}}\right], \qquad (2)$$

to improve the plume fitting. However, the governing equation (2) actually has not been verified by any measured data and thus its applicability remains obscure.

[4] To make this uncertainty even more complicated, *Zhang et al.* [2006a] found that there is an equally possible alternative fADE when the dispersion coefficient is space-dependent:

$$\frac{\partial C}{\partial t} = -\frac{\partial}{\partial x}[V(x)C] + \frac{\partial^{\alpha-1}}{\partial x^{\alpha-1}}\left[D(x)\frac{\partial C}{\partial x}\right]. \qquad (3)$$

However, some important information, including the quantitative distinction between these two fADEs, their underlying hydrogeological meanings and applicabilities to real data, and whether there might be other forms of physically possible fADEs, all remains unknown. The aim of this research is to provide the mathematical and physical basis of these possible extensions.

[5] The fADE is nonlocal by definition, since it describes the spread of solute mass over large distances via a convolutional fractional derivative. The coefficients may also vary locally in space, so that the strength of the nonlocal spreading may be a function of the local-scale subsurface heterogeneity. A fADE with space-dependent V and D therefore may extend the ability of the constant-parameter fADE to describe spatiotemporal plume behavior caused by the nonstationary distribution of subsurface heterogeneity. Similar to almost all modeling methods, knowledge of the variability of the local mean velocity should improve plume modeling. The same requirement can be found for the nonlocal continuous time random walks (CTRW), which typically focus on the retentive properties of the media [*Dentz et al.*, 2004]. A nonlocal transport equation (which is the scaling limit of the CTRW) containing hydrofacies-scale-dependent advection and dispersion is suggested by *Berkowitz et al.* [2002] to describe the influence of both the small- and regional-scale heterogeneities on solute transport. We take a similar philosophical approach with the spatial nonlocality here and investigate the derivation and application of a fADE with space-dependent parameters, for which a correct form has yet to be addressed systematically.

[6] This study focuses on the fADE with space-variable velocity and dispersion coefficient. In section 2, we evaluate and distinguish the two available forms, equations (2) and (3), and then explore another possible form of the fADE. The underlying physical meanings for all three fADEs are discussed, and efficient random walk approximations are developed. In section 3, we distinguish quantitatively all three fADEs by solving them numerically using both the implicit Euler method and the Lagrangian particle tracking method. In section 4, we test the applicability of the extended fADEs by using them to fit the tritium plumes measured at the MADE test site. Conclusions are drawn in section 5.

[7] The time-fractional ADE describing solute retention, and the multiscaling ADE describing direction-dependent superdiffusion, are discussed by *Schumer et al.* [2003a] and *Meerschaert et al.* [2001]. In this study, we restrict our attention to the one-dimensional, spatial fADE, since it is the most commonly used fADE at present, and the study of the one-dimensional case should provide a useful starting point to developing the physical model of the dynamics of particles in multiple dimensions [see *Zhang et al.*, 2006b]. Extensions to the time fractional and multiscaling cases will be discussed in a future paper.

2. fADEs With Space-Dependent Parameters

[8] The generalized mass balance law, using a fractional order of divergence between zero and unity [*Meerschaert et al.*, 2006], is used to derive the fADEs with space-dependent velocity V and dispersion coefficient D. The potential connection between the fADEs and the nonlocal dispersive constitutive models developed by *Cushman et al.* [1994] and *Neuman* [1993] is also discussed in Appendix A. To further elaborate on these fADEs, which provide Eulerian descriptions of solute flux, we establish a Lagrangian description of the dynamics of random-walking particles whose densities obey each fADE. Thus the differences between different fADEs can be seen from the different instantaneous motion of the particles. Also, note that in this study, we assume that the effective porosity of media is constant. The influence of the spatial variability of porosity on the process of anomalous diffusion will be discussed in a future paper.

2.1. Model 1: The FF-ADE

[9] A generalized Fick's law [*Paradisi et al.*, 2001; *Schumer et al.*, 2001; *Kim and Kavvas*, 2006] indicates that the dispersive flux F is proportional to a fractional derivative of solute concentration:

$$F = -D\frac{1+\beta}{2}\frac{\partial^{\alpha-1}C}{\partial x^{\alpha-1}} - D\frac{1-\beta}{2}\frac{\partial^{\alpha-1}C}{\partial(-x)^{\alpha-1}},$$

where β ($-1 \leq \beta \leq 1$) is the skewness. When $\alpha = 2$, this reduces to the classical Fick's law. To simulate super-Fickian dispersion in porous media, we anticipate that the largest particle motions are ahead of the mean velocity, so that $\beta = 1$ [see also *Schumer et al.*, 2001; *Zhang et al.*, 2006a] and thus the dispersive flux reduces to $F = -D\partial^{\alpha-1}C/\partial x^{\alpha-1}$. This term simulates faster-than-Fickian plume evolution through a permeability field with long-range dependence and high sample variance [*Herrick et al.*, 2002; *Grabasnjak*, 2003; *Trefry et al.*, 2003; *Kohlbecker et al.*, 2006]. The fractional order α decreases if the medium contains higher probabilities of high velocities.

[10] If we allow the strength of the above dispersive flux to be a function of x, then the traditional first-order mass conservation law results in the fADE (2) directly:

$$\frac{\partial C}{\partial t} = -\frac{\partial}{\partial x}\left[V(x)C - D(x)\frac{\partial^{\alpha-1}C}{\partial x^{\alpha-1}}\right]. \qquad (4)$$

We name equation (4) the "FF-ADE," where "FF" denotes the fractional flux, to distinguish it from the other fADEs discussed below. The FF-ADE (4) is also the same as the

fractional nonlinear Fokker-Planck equation suggested by *Tsallis and Lenzi* [2002]. However, this nonlinear equation does not seem to correspond to the forward equation of any Markov process (see the discussion by *Zhang et al.* [2006a]).

[11] To further explore the physical meaning underlying the fractional dispersive flux $-D(x)\partial^{\alpha-1}C/\partial x^{\alpha-1}$, we first expand the dispersive flux in equation (4) as

$$\frac{\partial}{\partial x}\left[D(x)\frac{\partial^{\alpha-1}C}{\partial x^{\alpha-1}}\right] = D(x)\frac{\partial^{\alpha}C}{\partial x^{\alpha}} + \frac{\partial D(x)}{\partial x}\frac{\partial^{\alpha-1}C}{\partial x^{\alpha-1}}, \qquad (5)$$

and then we approximate the α and $\alpha - 1$ order fractional derivative with a one-shift and zero-shift Grünwald formula, respectively [*Meerschaert and Tadjeran*, 2004]:

$$\frac{\partial^{\alpha}C(x,t)}{\partial x^{\alpha}} \approx \frac{1}{h^{\alpha}}\sum_{k=0}^{N}g_k C[x - (k-1)h, t], \qquad (6)$$

$$\frac{\partial^{\alpha-1}C(x,t)}{\partial x^{\alpha-1}} \approx \frac{1}{h^{\alpha-1}}\sum_{k=0}^{N-1}f_k C(x - kh, t), \qquad (7)$$

where h is the space step size, N is a sufficiently large number of grid points in the upstream direction, and g_k and f_k are the Grünwald weights

$$g_k = \frac{\Gamma(k - \alpha)}{\Gamma(-\alpha)\Gamma(k + 1)}, \qquad (8)$$

$$f_k = \frac{\Gamma[k - (\alpha - 1)]}{\Gamma[-(\alpha - 1)]\Gamma(k + 1)} = \frac{(k - \alpha)}{-\alpha}g_k. \qquad (9)$$

See also the study by *Miller and Ross* [1993, chapter 2] for the "standard" Grünwald approximation and the associated weights. In the one-shift Grünwald approximation for $\partial^{\alpha}C/\partial x^{\alpha}$, the only negative term in the sequence of Grünwald weights g_k is $g_1 = -\alpha$, while in the zero-shift Grünwald approximation for $\partial^{\alpha-1}C/\partial x^{\alpha-1}$, the only positive term in the sequence of Grünwald weights f_k is $f_0 = 1$. The weights g_k (or f_k) sum to zero. Also, note that when $\alpha = 2$, the one-shift Grünwald approximation (6) reduces to the second-order central difference, and the zero-shift Grünwald approximation (7) reduces to the backward first difference.

[12] A finite distribution of g_{k+1} and f_k, which signifies the contribution of concentration from upstream nodes, is shown in Figure 1. On the basis of equations (6) and (7), the total weight assigned at one grid point to an upstream concentration $C(x - kh, t)$ is $w(k) = D(x)g_{k+1}/h + [\partial D(x)/\partial x]f_k/h^{\alpha-1}$, which may vary significantly with x. In the original fADE (1), however, the distribution of weights does not change with x because of the constant D. The weight at location $x - kh$, which is $w(k)' = Dg_{k+1}/h^{\alpha}$ (as shown by the triangles in Figure 1 for a specific example), is also quite different from the weight $w(k)$ for the FF-ADE (as shown by the crosses in Figure 1). In equation (5), both the $D(x)$ and the $\partial D(x)/\partial x$ are evaluated at the current location (local) x, not the value at any upstream (nonlocal) zone.

[13] The expansion (5) implies that only the spatial variation in $D(x)$ and its first derivative affect the solute
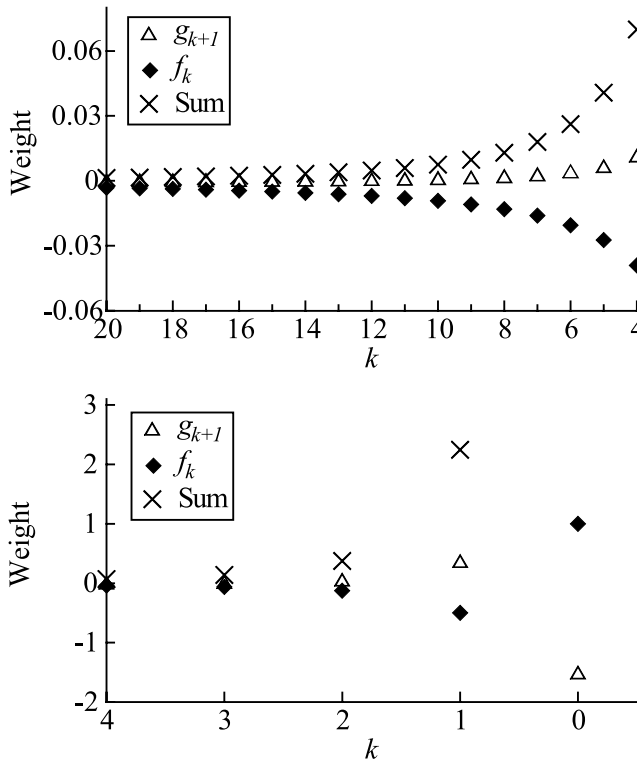
Figure 1. Distribution of Grünwald weights g_{k+1} and f_k with the scale index $\alpha = 1.5$. For clarity, two figures are used to show different ranges of k. The symbol "Sum" represent the summation of weights in equations (6) and (7), which is $D(x)g_{k+1}/h^\alpha + [\partial D(x)/\partial x]f_k/h^{\alpha-1}$. The space step size $h = 1$, so here $g_{k-1} = g_{k-1}/h^\alpha$ and $f_k = f_k/h^{\alpha-1}$. In "Sum," $D = 6$ and $\partial D/\partial x = 0.01$.

transport. Interestingly this formulation makes the FF-ADE (4) difficult to approximate by a Markovian process [also see *Zhang et al.*, 2006a]. Only for the specific case where D is linear will the FF-ADE (4) correspond to a Markov process. In this case (no matter the properties of velocity V), the FF-ADE (4) can be solved by the random-walk particle tracking method where an individual particle moves based on the following Langevin equation [*Zhang et al.*, 2006a]

$$\mathrm{d}X(t) = V\,\mathrm{d}t + D^{\frac{1}{\alpha}}\mathrm{d}L_\alpha(t) + \Theta(\alpha-1)^{\frac{1}{\alpha-1}}\left|\frac{\partial D}{\partial x}\right|^{\frac{1}{\alpha-1}}\mathrm{d}L_{\alpha-1}(t), \quad (10)$$

where $\mathrm{d}L_\alpha(t)$ and $\mathrm{d}L_{\alpha-1}(t)$ denote independent random noises underlying an α-order and $(\alpha - 1)$-order Lévy motion (independent of the initial location X_0), respectively, and $\Theta = \mathrm{sign}(\partial D/\partial x)$ denotes the sign function where $\Theta = -1$ if $\partial D/\partial x > 0$ and -1 otherwise. The $(\alpha - 1)$-order Lévy random noise scaled by the gradient of the dispersion coefficient, as indicated by the third term on the right-hand side (RHS) of equation (10), captures the influence of the spatial variation of dispersion coefficient on the drift of solutes. This compares directly to the additional drift that arises from $\mathrm{d}D(x)/\mathrm{d}x$ in the traditional ADE [*LaBolle et al.*, 1996]. If the effective porosity also varies in space, then the spatial variability in porosity will also affect the drift, but not the dispersion [*LaBolle and Zhang*, 2006].

2.2. Model 2: The FD-ADE

[14] If the dispersive flux $-D(x)\frac{\partial^{\alpha-1}C}{\partial x^{\alpha-1}}$ in equation (4) is replaced by a new form $-\frac{\partial^{\alpha-2}}{\partial x^{\alpha-2}}[D(x)\frac{\partial C}{\partial x}]$, we get the fADE (3) using the first-order mass conservation law

$$\begin{aligned}\frac{\partial C}{\partial t} &= -\frac{\partial}{\partial x}\left\{V(x)C - \frac{\partial^{\alpha-2}}{\partial x^{\alpha-2}}\left[D(x)\frac{\partial C}{\partial x}\right]\right\}\\ &= -\frac{\partial}{\partial x}[V(x)C] + \frac{\partial^{\alpha-1}}{\partial x^{\alpha-1}}\left[D(x)\frac{\partial C}{\partial x}\right].\end{aligned} \quad (11)$$

See also the multidimensional form derived by *Meerschaert et al.* [2006]. The $(\alpha - 2)$-order fractional derivative is actually a fractional integral. The net inflow of dispersive flux in equation (11) represents a fractional divergence (the concept of fractional divergence is given by *Meerschaert et al.* [2006] and it will be introduced briefly in the next subsection), so we name it "FD-ADE," where "FD" denotes the fractional divergence. Note that the dispersive flux in equation (11) is closely related to the adjoint of the dispersive flux in the FF-ADE (4) [*Feller*, 1971; *Zhang et al.*, 2006a]:

$$\left\{\frac{\partial}{\partial x}\left[D(x)\frac{\partial^{\alpha-1}C}{\partial x^{\alpha-1}}\right]\right\}^* = -\frac{\partial^{\alpha-1}}{\partial(-x)^{\alpha-1}}\left[D(x)\frac{\partial C}{\partial x}\right],$$

where the superscript * indicates the adjoint operator.
[15] Here the net inflow of dispersive flux into the small control volume of porous media at x is a value weighted by dispersive fluxes at all upstream zones. It can be approximated by

$$\begin{aligned}\frac{\partial^{\alpha-1}}{\partial x^{\alpha-1}}\left[D(x)\frac{\partial C(x,t)}{\partial x}\right] &\approx \frac{1}{h^{\alpha-1}}\sum_{k=0}^{N-1}f_k\left[D(x-kh)\right.\\ &\left.\times\frac{C(x-(k+1)h,t) - C(x-kh,t)}{h}\right].\end{aligned} \quad (12)$$

Therefore the dispersive flux at any upstream zone $y < x$ can reach x, and thus all particles arriving at x retain their memory of both the D value at the upstream point y and the gradient of concentration along the way. Both the concentration gradient and the dispersion coefficient are nonlocal. This makes the FD-ADE (11) physically different from the FF-ADE (4).
[16] One can also expand the net dispersive flux in equation (11) using the fractional Leibniz rule [*Osler*, 1971] into an infinite series of fractional derivatives and integrals

$$\begin{aligned}\frac{\partial^{\alpha-1}}{\partial x^{\alpha-1}}\left[D(x)\frac{\partial C}{\partial x}\right] &= \sum_{n=0}^{\infty}\binom{\alpha-1}{n}\frac{\partial^n D(x)}{\partial x^n}\frac{\partial^{\alpha-n}C}{\partial x^{\alpha-n}},\\ \text{where }\binom{\alpha}{n} &= \frac{\Gamma(1+\alpha)}{\Gamma(1+\alpha-n)n!}.\end{aligned}$$

Thus the FD-ADE (11) with $1 < \alpha < 2$ does not ignore the influence of nonlinearities of $D(x)$ on solute transport. It can be solved by a particle tracking scheme based on the following Markov process [*Zhang et al.*, 2006a]

$$\mathrm{d}X(t) = V\,\mathrm{d}t + D^{\frac{1}{\alpha}}\mathrm{d}L_\alpha(t) + \Theta\left|\frac{\partial D}{\partial x}\right|^{\frac{1}{\alpha-1}}\mathrm{d}L_{\alpha-1}(t), \quad (13)$$

for any functional forms of velocity and dispersion coefficient as long as the dispersion coefficient is first-order differentiable.

[17] The difference between the FD-ADE and the FF-ADE can also be seen clearly from their corresponding Markov processes in the special cases where they exist. When $D(x)$ increases linearly in space, the solute transport captured by the FF-ADE has less additional drift than the FD-ADE, by a factor $(\alpha - 1)^{1/(\alpha-1)}$, as indicated by the last term on the RHS of the Markov processes (10) and (13). The opposite is true when D decreases linearly in space. However, if the solute transport is advection-dominated [which means the first term on the RHS of equations (10) or (13) is dominant] and the dispersion coefficient is relatively smooth in space [which means $D \gg \partial D/\partial x$ in equations (10) and (13)], the FD-ADE should produce results very similar to the FF-ADE. We test these qualitative conclusions numerically in section 3.

2.3. Model 3: The FFD-ADE

[18] The fractional derivative version of the divergence developed by *Meerschaert et al.* [2006] yields the following generalized continuity equation (mass conservation law)

$$\partial C/\partial t = -\mathrm{div}^{\gamma}\mathbf{F},\qquad(14)$$

where the symbol "div" denotes the divergence, $\mathbf{F}$ denotes the classical integer-order (or local) flux, and $0 < \gamma < 1$. The quantity $\mathrm{div}^{\gamma}\mathbf{F}$ is understood in terms of its Fourier transform $\int (i\mathbf{k}\cdot\theta)^{\gamma}\hat{\mathbf{F}}(\mathbf{k})\cdot\theta\,M(\theta)\mathrm{d}\theta$, where $M(\theta)$ is an arbitrary density function on the unit sphere. In a one-dimensional case, if particle motions are restricted to the downstream direction only, one has $M(\theta) = 1$ for $\theta = +1$, and $M(\theta) = 0$ for $\theta = -1$. Therefore the quantity $\mathrm{div}^{\gamma}\mathbf{F}$ reduces to $(ik)^{\gamma}\hat{\mathbf{F}}(k)$ in Fourier space. When $\gamma = 1$ and the flux is advection and Fickian dispersion, the above continuity equation reduces to the classical ADE.

[19] In order to compare directly with the previous fADEs, we wish to have an α-order dispersion term, so we let the order of mass conservation $\gamma = \alpha - 1$. Thus we get the following fADE which has not previously been considered:

$$\begin{aligned}\frac{\partial C}{\partial t} &= -\frac{\partial^{\alpha-1}}{\partial x^{\alpha-1}}\left[V(x)C - D(x)\frac{\partial C}{\partial x}\right]\\ &= -\frac{\partial^{\alpha-1}}{\partial x^{\alpha-1}}[V(x)C] + \frac{\partial^{\alpha-1}}{\partial x^{\alpha-1}}\left[D(x)\frac{\partial C}{\partial x}\right].\end{aligned}\qquad(15)$$

It contains fully fractional divergence, so we denote this equation "FFD-ADE" (where "FFD" represents the fully fractional divergence) to distinguish it from the FD-ADE (11) with fractional divergence in only the dispersive term.

[20] Similar to equation (11), if the total flux is nonlocal with the form

$$q(x,t) = \frac{\partial^{\alpha-2}}{\partial x^{\alpha-2}}\left[V(x)C - D(x)\frac{\partial C}{\partial x}\right],\qquad(16)$$

then a classical mass balance law results in the FFD-ADE (15) as well. Therefore the classical mass balance of nonlocal total flux is mathematically equivalent to the fractional-order mass balance of local total flux. They both show that the resultant net advective and dispersive fluxes may be nonlocal.

[21] When V is constant, the nonlocal advective flux in equation (16) with the form $\frac{\partial^{\alpha-2}}{\partial x^{\alpha-2}}[V(x)C]$ reduces to $V\partial^{\alpha-2}C/\partial x^{\alpha-2}$, which is a special case of the nonlocal constitutive theory with the advective travel distance much larger than the scales of heterogeneity (see Appendix A). A similar time nonlocality of advective flux was used recently by *Dentz and Tartakovsky* [2006], where the delay in the advective flux was assumed to be caused by variable porosity and adsorption properties of the porous media, as well as trapping in relatively immobile domains. It is noteworthy that their delay mechanism is also a special case (i.e., local spatial version) of the preasymptotic dispersive flux (A1) proposed by *Cushman et al.* [1994].

[22] The FFD-ADE (15) can be approximated by the following generalized Langevin equation containing three independent Lévy random noises (see Appendix B):

$$\mathrm{d}X(t) = V^{\frac{1}{\alpha-1}}\mathrm{d}L_{\alpha-1}(t) + D^{\frac{1}{\alpha}}\mathrm{d}L_{\alpha}(t) + \Theta\left|\frac{\partial D}{\partial x}\right|^{\frac{1}{\alpha-1}}\mathrm{d}\tilde{L}_{\alpha-1}(t).\qquad(17)$$

The FFD-ADE (15) is similar to the FD-ADE (11) except that the net advective flux is nonlocal. In other words, the drift of solutes has an infinite upstream memory of both velocity and concentration. It corresponds to an aquifer with regional-scale, high-permeable preferential flow paths, where the upstream advective fluxes may affect the local advective flux at all downstream zones. Thus it allows the plume to migrate with a relatively faster rate than in the FF-ADE (4) and the FD-ADE (11). In the latter two cases, the solute can only disperse preferentially at velocities ahead of the mean groundwater velocity, causing the plume peak to lag behind that of either the FFD-ADE (15) or the classical second-order case [*Schumer et al.*, 2003a]. In certain depositional environments such as the typically alluvial or glacial-fluvial aquifer systems, the high-permeable ancient channel deposits tend to form regional-scale preferential flow paths for water and solutes. As soon as the solute enters into these three-dimensional "tubes," the plume front or plume peak may move much faster than the Gaussian case. One possible physical description of this transport phenomenon is that the advective travel distance is much larger than the scales of heterogeneity [as expressed by equation (A12) in Appendix A3], and thus one possible way to simulate this process is to use the FFD-ADE.

[23] Note that when $\alpha = 2$, all of the above fADEs [equations (4), (11), and (15)] reduce to the second-order ADE (if the upstream boundary remains clean from the contaminants in the last two fADEs), and all above Markov processes [equations (10), (13), and (17)] reduce to the traditional Markov process used to simulate the second-order ADE [*LaBolle et al.*, 1996, 1998].

3. Numerical Distinction of the fADEs

[24] We illustrate further the difference and similarity of these fADEs by solving them numerically with both the implicit Euler finite difference method and the Lagrangian random-walk particle tracking method. Numerical methods are developed in this study because analytical solutions are unavailable for the variable coefficient fADEs.

[25] The implicit Euler finite difference solution for the FF-ADE (4) discussed by *Zhang et al.* [2006a] can be

Table 1. Parameters Used for Four Numerical Scenarios[a]

Scenarios	D, m$^\alpha$/d	V	α	Initial Location, m
Scenario 1	$0.06x$	$0.1x$	1.7	25
Scenario 2	$0.06x$	$0.1x$	1.9	25
Scenario 3	$0.1x$	$0.001x$	1.5	50
Scenario 4	$0.1x$	$0.001x$	1.9	50

[a]x denotes the coordinate, and $x \geq 0$ in section 3. The units of V are m/d for the original fADE (1), the FF-ADE (4), and the FD-ADE (11), and m$^{\alpha-1}$/d for the FFD-ADE (15).

extended to the FD-ADE (11) and FFD-ADE (15). The shifted Grünwald formula proposed by *Meerschaert and Tadjeran* [2004] is used to approximate the fractional derivatives embedded in these fADEs [for instance, see equations (6) and (7)]. The stability requirement for the finite difference scheme solving the FF-ADE (4) was analyzed by *Zhang et al.* [2006a], and the other cases are similar.

[26] The random walk method is used in this study, since it may be the method of choice for simulating anomalous transport described by the above fADEs through large flow systems in heterogeneous porous media or fracture networks, as is the case for the second-order ADE. In particular, the random walk method is the only known way at present to simulate the multiscaling anomalous diffusion process through nonhomogeneous systems [*Zhang et al.*, 2006b].

3.1. Linear D

[27] Four scenarios (Table 1), where D and V vary linearly in space, are selected to show the influences of the fractional dispersivity (defined by D/V) and the scale index on solute transport captured by each fADE, as discussed qualitatively above. We first solved each fADE with the random-walk particle tracking method by simulating individual particle motion using the Markov processes listed above. We then solved each fADE with the implicit Euler finite difference method as a cross-verification. In the four scenarios we selected, the first two are highly advection dominated ($\|D\| = 0.6\|V\|$, where $\|D\|$ and $\|V\|$ denote the magnitude of D and V), while the last two are dispersion dominated ($\|D\| = 100\|V\|$). The length and time units are consistent between D and V. In particular, with $\alpha = 1.9$ and $\|D\| = 100\|V\|$, the last scenario is the most Fickian-like for the FFD-ADE (15).

[28] In all scenarios, the FD-ADE (11) has a slightly larger drift than the FF-ADE (4) when the dispersion coefficient increases linearly with distance. The direction of the additional drift is along the direction of the increase of dispersion coefficient, and the relative magnitude of this drift increases with an increase of the fractional dispersivity. As expected, when $\|\partial D/\partial x\| \ll \|D\|$ (such as scenarios 1 and 2 in Table 1), the FF-ADE (4) and the FD-ADE (11) capture almost identical plume behavior (Figures 2a and 2b). On the other hand, the difference between the FFD-ADE and the FF/FD-ADE increases when the system is more advection dominated (i.e., when the fractional dispersivity is relatively small) and/or the scale index decreases (Figures 2a and 2b). When the flow is advection dominated (such as scenarios 1 and 2), the FFD-ADE describes the fastest plume peak and the heaviest leading tail, since the FFD-ADE captures the highest nonlocality of advective flux.

[29] We then investigated the breakthrough curve (BTC) in scenario 1 (Figure 3). In this case, where the solute transport

is advection dominated, the BTC peak described by the FFD-ADE arrives three times earlier than that described by the FD-ADE, and the BTC peak value described by the FFD-ADE is an order-of-magnitude lower than that described by the FD-ADE. The FF-ADE has an almost identical BTC as
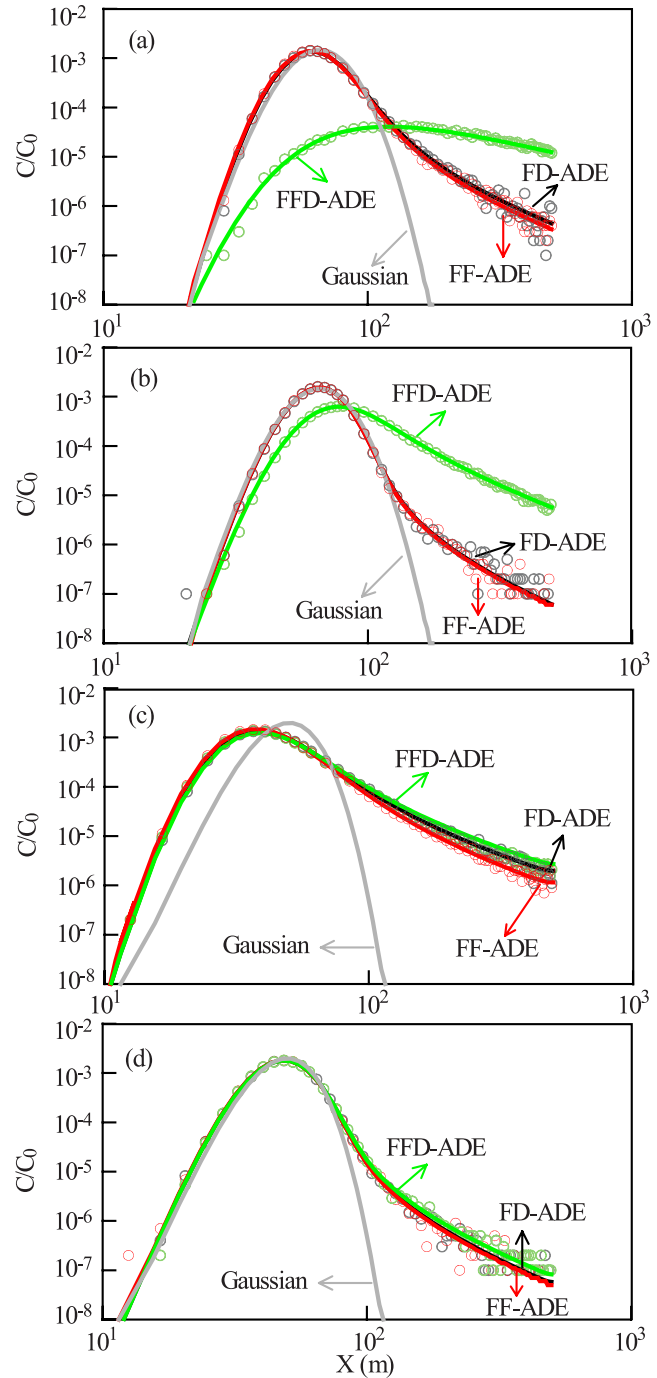

Figure 2. Simulated resident concentrations described by the FF-ADE (4) (gray thin lines), the FD-ADE (11) (dark thin lines), and the FFD-ADE (15) (thick solid lines) in scenarios (a) 1, (b) 2, (c) 3, and (d) 4. The symbols represent the random-walk particle tracking approximations, and the solid lines represent the solutions of implicit Euler finite difference method. The Gaussian solution is also shown for comparison. The instantaneous source is injected at the initial point shown in Table 1. The running time is 10 days.
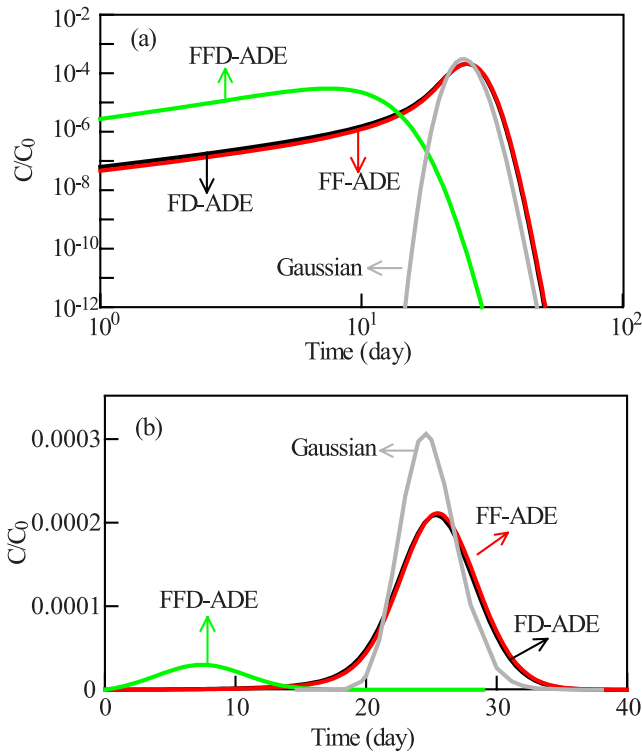
Figure 3. Simulated breakthrough curves at $x = 300$ m for all fADEs in scenario 1. The Gaussian case is also shown for the purpose of comparison. (a) Log-log plot; (b) linear-linear plot.

the FD-ADE. In a log-log plot, the slopes of the early tail of BTCs described by all fADEs are similar. These early breakthrough lines have a 1:1 slope on a log-log plot. Additionally, as expected, the BTC peaks of the FD-ADE and the FF-ADE arrive very slightly behind that of the Gaussian case, since the fADEs have more mass in front of the peak.

3.2. Nonlinear D

[30] As discussed previously, the FD-ADE (11) considers all nonlinearities of D at the local point x, distinguishing it from the FF-ADE (4). To illustrate the effect, we simulated the resident concentrations caused by a nonlinear $D(x) = 10^{-3}x^{1.4}$ m$^{1.4}$/d (Figure 4a). As the dispersion coefficient grows, the FD-ADE (11) results in greater mass in the leading edge.

[31] When D is spatially nonlinear, the dispersion in the FD-ADE (11) contains an infinite series of terms, which can be written as

$$\frac{\partial^{\alpha-1}}{\partial x^{\alpha-1}}\left[D(x)\frac{\partial C(x,t)}{\partial x}\right] = D(x)\frac{\partial^{\alpha}C}{\partial x^{\alpha}} + (\alpha-1)\frac{\partial D(x)}{\partial x} \times \frac{\partial^{\alpha-1}C}{\partial x^{\alpha-1}} + \sum_{n=2}^{\infty}\frac{\Gamma(\alpha)}{\Gamma(\alpha-n)n!}\frac{\partial^{n}D(x)}{\partial x^{n}}\frac{\partial^{\alpha-n}C}{\partial x^{\alpha-n}}. \tag{18}$$

Here we explore the contributions to solute concentration from each of the three terms on the RHS of the above equation. The first case (denoted as case 1 in Figure 4b) includes only the first term, $D(x)\frac{\partial^{\alpha}C}{\partial x^{\alpha}}$. The second case (case 2) includes the first two dispersive terms, and the third case (case 3) contains all terms.

[32] The results (Figure 4b) show that the first term on the RHS, $D\partial^{\alpha}C/\partial x^{\alpha}$, dominates the solution. The other terms, containing different orders of spatial derivative of D (note that the term $\partial^{\alpha-n}C/\partial x^{\alpha-n}$ becomes a fractional integral when the fractional order of derivative, $\alpha - n$, is negative), reduce mass in the leading edge. Their contribution to the solute decreases quickly with an increase in n, corresponding to an increase in the order of the derivative and a reduction in their coefficients, $\Gamma(\alpha)/\Gamma(\alpha - n)n!$. Therefore the reason that the FD-ADE (11) has a more apparent leading edge than the FF-ADE (4) is because the weight $(\alpha - 1)$ of the first-order derivative of D is less than that of the FF-ADE, which is 1.
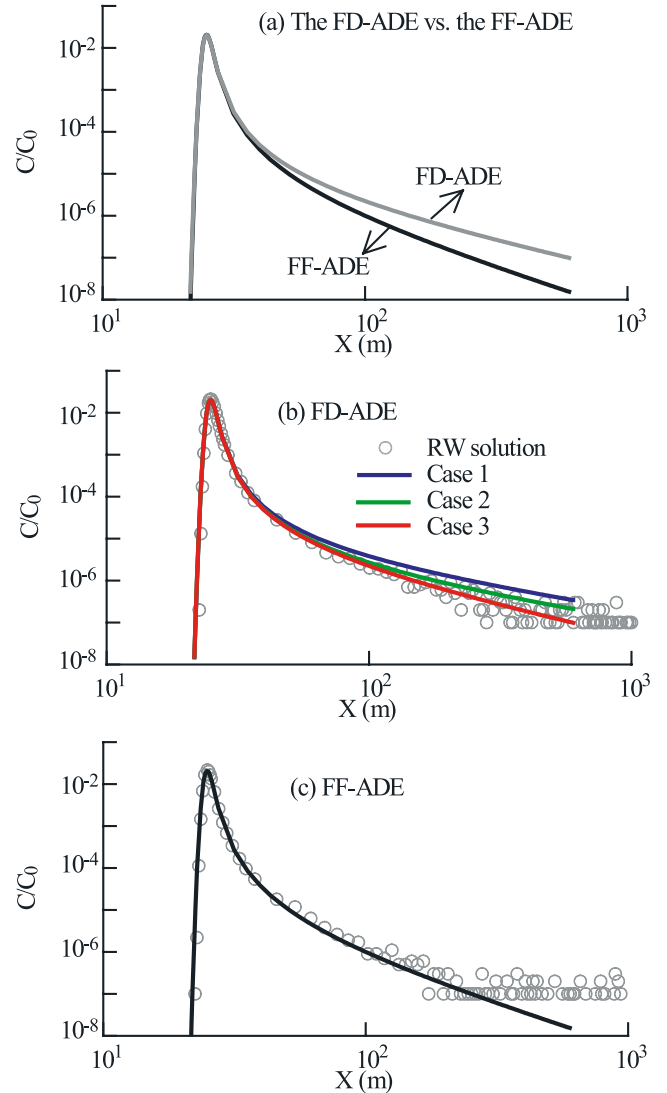

Figure 4. Simulated resident concentration for a nonlinear $D(x) = 10^{-3} \times x^{1.4}$ m$^{1.4}$/d, $V(x) = 10^{3} \times x^{1.4}$ m/d, and an instantaneous point source is located at $x_0 = 25$ m. The running time is 10 days, and $\alpha = 1.4$. (a) Implicit Euler finite difference solutions for the FD-ADE versus the FF-ADE. (b) Contribution of each dispersive term for the FD-ADE. Case 1 considers D only, case 2 considers both D and $\partial D/\partial x$, and case 3 is a complete version of the FD-ADE (11). The circles denote the RW approximations. (c) RW approximations (circles) using (10) versus the finite difference solutions (line) for the FF-ADE (4).

Note that this conclusion will be opposite if D decreases in the direction of travel (such as in radial diverging tests). It also explains why the discrepancy between these two fADEs becomes more apparent with the decrease of the scale index α.

[33] Since the influences of high-order derivatives of D on plume transport are weak compared to that of D and its gradient, the Markov process (10) which gives an exact particle tracking solution in the case of a linear D term may also be used as a reasonable approximation for the FF-ADE (4) with a nonlinear D. A demonstration is shown in Figure 4c. Process (10) explicitly captures the dispersion caused by both D and its gradient, while the corresponding fractional Fokker-Planck equation of (10) with a nonlinear D contains other high-order derivatives of D [*Zhang et al.*, 2006a]. Hence we conclude that both the FD-ADE and the FF-ADE can be simulated with reasonable accuracy with the simple random walk formulations (13) and (10), respectively. However, if D contains stronger nonlinearity than that discussed above, we suggest similar numerical tests for users who approximate the FF-ADE (4) using the Markov process (10).

4. Application: The MADE Site Revisited

[34] Given the physical and mathematical distinction of the three fADEs discussed above, we still cannot determine which form to use for a specific site given the usually limited information about subsurface heterogeneity. Fortunately, the FD-ADE and the FF-ADE forms, which are based on very different mass balance equations, yield very similar results for certain conditions [i.e., relatively smooth $D(x)$]. Furthermore, the FFD-ADE (15) has an easily identifiable heavier leading edge and faster spreading rate. However, the only reliable way for equation selection and parameter estimation may be the field application and numerical testing of these fADEs with real data. In this section, we apply all three fADEs to fitting the tritium plumes measured at the MADE test site.

4.1. Anomalous Transport and Previous Modeling Methods

[35] The natural-gradient tracer tests conducted from 1986 to 1997 at the Columbus Air Force Base in northeastern Mississippi, commonly known as the MADE site, have addressed continuous interest, probably because of the strong influence of "high" subsurface heterogeneity on solute transport [*Boggs et al.*, 1992; *Adams and Gelhar*, 1992; *Boggs and Adams*, 1992]. The MADE site has a variance of log conductivity [ln(K)] as high as 4.5 [*Rehfeldt et al.*, 1992], which is much larger than previous natural gradient experiment sites, including the Borden site (0.29 [see *MacKay et al.*, 1986]), the Cape Cod site (0.26 [see *Garabedian*, 1987; *LeBlanc et al.*, 1991]), and the Twin Lake site (0.031 [see *Killey and Moltyaner*, 1988]). However, *Fogg* [2004] showed that a 4.5 variance of ln(K) is not uncommon, especially for large alluvial aquifer systems. The MADE site aquifer is dominated by unconsolidated sand and gravel, with less clay and silt deposits which might form the relatively immobile, irregular lenses and layers [*Rehfeldt et al.*, 1992]. In typical alluvial depositional systems, the high-K paleochannel sands and gravels tend to be interconnected in space (as long as their volume

fraction is sufficiently large) and thus provide multiscale preferential flow paths for water and solute [*Fogg et al.*, 2000]. The surrounding (for a fine-grain-dominated system) or embedded (for a coarse-grain-dominated system) low-K sediments sequester the solutes, especially near the source [*LaBolle and Fogg*, 2001]. This can result in a positively skewed, anomalous or non-Fickian dispersion affecting both the near-source peak and the downstream front, both of which were observed at the MADE site and cannot be fitted by the classical ADE with a coarse-scale flow field [*Adams and Gelhar*, 1992].

[36] The plausible hydrogeological explanation for the "nonideal" transport behavior observed at the MADE site supports three types of modeling methods, which include the following: (1) the second-order ADE with a fine-scale velocity field capturing both the multiscale flow paths and relatively immobile, trapping zones [*Zheng and Jiao*, 1998; *Eggleston and Rojstaczer*, 1998; *Zheng and Gorelick*, 2003; *Zinn and Harvey*, 2003; *Liu et al.*, 2004]; (2) the dual-domain approach with a relatively coarse (upscaled) flow field [*Harvey and Gorelick*, 2000; *Feehley et al.*, 2000; *Julian et al.*, 2001]; and (3) novel nonlocal techniques, such as the CTRW method [*Berkowitz and Scher*, 1998] and the fADE method [*Benson et al.*, 2001], which directly capture the anomalous transport process, using a very coarse, or even a constant, mean transport velocity. An exceptional case of the first method was discussed recently by *Barlebo et al.* [2004], who showed that the second-order ADE with a simplified zonal conductivity (K) field can also characterize the positively skewed plume at the MADE site. However, *Molz et al.* [2006] argued that a large and unrealistic K was assigned for the zone at the downstream plume front by *Barlebo et al.* [2004] to produce the fast leading edge. Nevertheless, the practicality of the first method is questionable, as research implies that the scale of the flow field needed for its application might be too fine to be characterized sufficiently by current techniques and available information. The tradeoff between the dual-domain approach (either a single rate or multirate method) and the flow field remains an open research question (see the conclusion of *Hill et al.* [2006]). Therefore the third method may be the most computationally efficient at present and deserves further study, although the one-dimensional fADE with constant parameters [based on equation (1)] does not capture all of the three-dimensional features of the MADE site tritium plume, as noted by *Lu et al.* [2002]. The applicability of the CTRW method in capturing the heavy leading edges of the MADE site plumes is beyond the scope of this study, and we will show the details in a future paper.

4.2. Application of the fADEs (1), (4), (11), and (15)

[37] A motivation of this study is to improve the predictive ability of the fADE. To compare directly to the results of a previous constant parameter fADE method developed by *Benson et al.* [2001], we fit the same one-dimensional projected, mass-normalized relative concentrations of tritium measured at the MADE-2 test site. The drop in mobile mass due to long-term retention may be modeled by a separate process that can easily be added [*Schumer et al.*, 2003b].

[38] First we refit the MADE-2 tritium plumes using the original fADE (1) with constant parameters to identify its possible insufficiency. There were four snapshots measured at days 27, 132, 224, and 328, respectively. The first plume
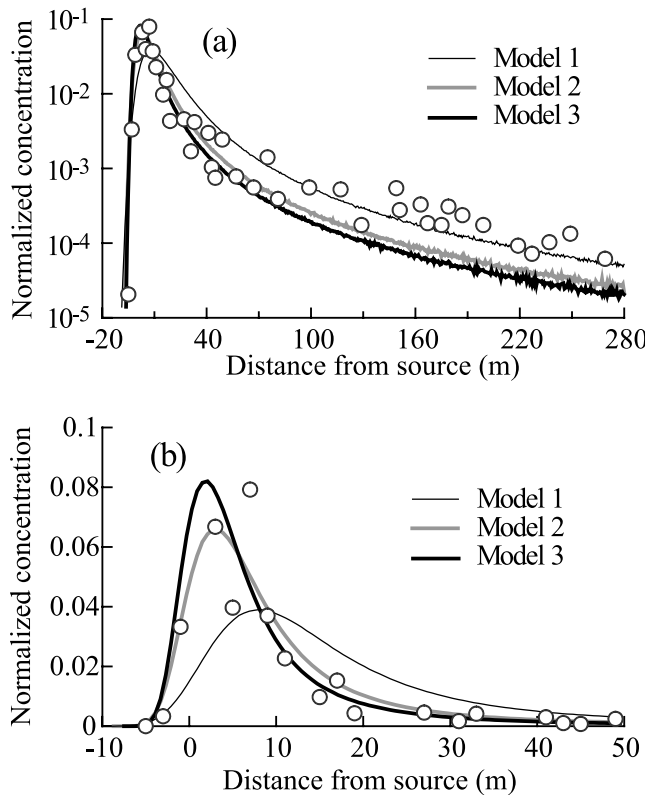
Figure 5. (a) Semilog and (b) linear plots of the measured (circles) versus the simulated (lines) resident concentrations using the original fADE (1) with a mean velocity V and a scale-independent dispersion coefficient D, of the MADE-2 tritium at day 224. The scale index $\alpha = 1.1$. $V = 0.25$ m/d and $D = 0.25$ m$^{1.1}$/d for model 1, $V = 0.14$ m/d and $D = 0.14$ m$^{1.1}$/d for model 2, and $V = 0.11$ m/d and $D = 0.11$ m$^{1.1}$/d for model 3.

at day 27 looks more like a "normal" (Gaussian) one [see *Benson et al.*, 2001] and deviates significantly from others, possibly because of the radial flow field induced by the initial 48.5-hour injection of tracer source, the limited samples collected from wells near the source (the sampling wells at day 27 are no further than 27.2 m from the injection source), and/or the truncation of the leading edge with its concentration lower than the detection limit or the background level. The second plume at day 132 was somewhat truncated (i.e., "lost" its leading edge) during the measurement cycle, as discussed by *Lu et al.* [2002]. The sampling wells at day 132 are no further than 85.4 m from the injection source, while the leading edge appears to be longer. The sampling wells were extended to 276.1 m for the following measurement cycles, where the leading edge was found at the farthest well. Therefore the last two snapshots may be relatively more complete and reliable, and thus we restrict our attention to them. Calculated concentrations at day 224 (Figure 5) show that the original fADE (1) with a mean velocity V and a scale-independent dispersion coefficient D can accurately capture either the near-source peak or the downstream front, but slightly underestimates one or the other. The same conclusion can be found for day 328 (not shown). This is consistent with the finding of *Lu et al.* [2002]. The best fit model based on equation (1) has parameters (listed in Table 2) very close to

the parameters predicted from the K statistics listed by *Benson et al.* [2001]. The resultant sum of the squared difference (SSD) between the natural logarithms of the predicted and observed concentrations is also shown in Table 2. Note that the SSD can only provide a very coarse criterion about the model fitting considering the noise in the projected one-dimensional plume.

[39] The fits can be improved by using the FF-ADE (4) or FD-ADE (11), where the parameters are allowed to be space-dependent to capture the local variation of the spreading of plumes. The aquifer material is reportedly different along the length of the plume [*Boggs et al.*, 1992; *Adams and Gelhar*, 1992; *Rehfeldt et al.*, 1992]. For simplicity, here we assume that the mean velocity V is constant and the dispersion coefficient D, which is a measure of velocity deviations, varies linearly with transport distance. The best fit parameters are listed in Table 2. Both the FF-ADE (4) and the FD-ADE (11) improve the fitting of both the peak and the leading tail compared to the original fADE (1) (Figure 6).

[40] The FFD-ADE (15) with constant parameters can capture the positively skewed plume with near-source peak and heavy leading tail (see Table 2 and Figure 6). Note here that the best fit scale index ($\alpha = 1.6$) is much larger than the value for other fADEs, while the velocity and dispersion coefficient are much smaller than those of other fADEs. We discuss this discrepancy below.

4.3. Discussion

[41] The FD-ADE (11) captures the leading edge slightly better than the FF-ADE (4), although its SSD is slightly larger. As discussed above (see the numerical results and analysis in section 3), the FD-ADE (11) exhibits more drift than the FF-ADE (4), since the scale index is low ($\alpha = 1.1$) and the advection is relatively large at the MADE site. The FD-ADE describes a slightly heavier leading tail than the FF-ADE does, although the FD-ADE uses smaller velocity and dispersion coefficient (Table 2). The fits are very similar, and considering the fact that the FD-ADE (11) can be solved more efficiently by random walks compared to the FF-ADE (4), we suggest the use of the FD-ADE at the MADE site. We also note that all of the parameters in both the FD-ADE and FF-ADE are consistent with the analysis of the K statistics by *Benson et al.* [2001]. Furthermore, analysis of the depositional history suggests that the central portion of the test site surface may correspond with a former river meander, which has distinct hydraulic properties compared to the materials deposited near the source area where the tracers were injected [*Rehfeldt et al.*, 1992]. This motivates us to build a zonal-parameter model, containing as few parameters as possible, to replace the relatively more

Table 2. Calibrated Parameters and the Resultant Sum of the Squared Difference (SSD) Between the Natural Logarithms of the Predicted and Observed Concentrations at the MADE Site Using Each fADE[a]

fADEs	V	D, m$^{\alpha}$/d	α	SSD, 224d	SSD, 328d
fADE (1)	0.14	0.14	1.1	7.68	10.78
FF-ADE (4)	0.195	$0.006x + 0.2$	1.1	2.19	5.27
FD-ADE (11)	0.114	$0.00158x + 0.11$	1.1	2.21	6.06
FFD-ADE (15)	0.012	0.009	1.6	1.54	6.74

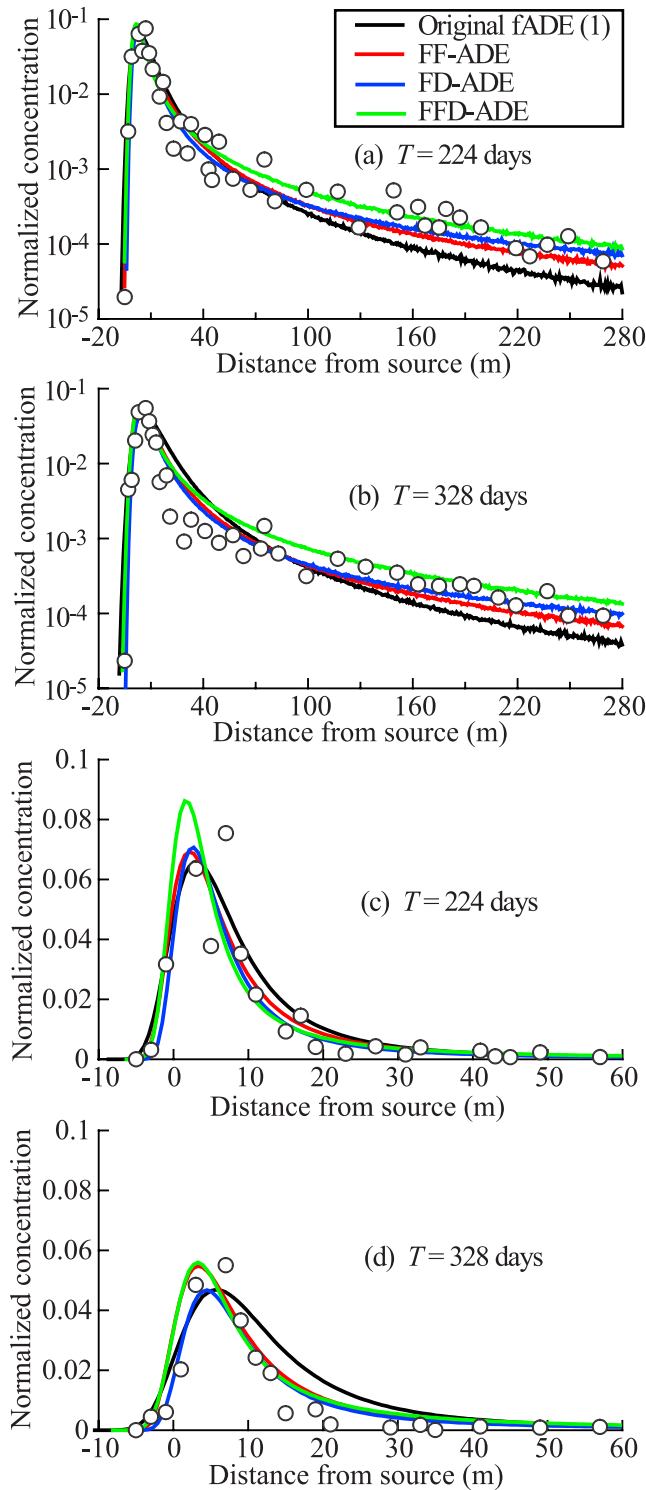[a]The units of V are the same as those used in Table 1.

Figure 6. Measured (circles) versus the simulated (lines) resident concentrations using the original fADE (1), the FF-ADE (4), the FD-ADE (11), and the FFD-ADE (15) for (a) day 224 and (b) 328. (c, d) Linear plots of Figures 6a and 6b. Parameters are shown in Table 2.

complex model discussed above. Such a model is theoretically and practically much easier to define and calibrate. Once again, we assume constant V so that the one-dimensional flow field is divergence-free and conserves mass. We then allow D to increase to account for the greater differential

velocities. A two-dimensional model should allow V and D to vary, possibly simultaneously.

[42] We recalculated the tritium resident concentration by building a simplified, two-zone model. The FD-ADE (11) was selected as a demonstration. The dispersion coefficient $D = 0.14$ m$^{1.1}$/d for $x < 40$ m and $D = 0.30$ m$^{1.1}$/d for $x \geq 40$ m, while the velocity $V = 0.14$ m/d remains constant in space. This simple model can capture the near-source peak and the downstream front simultaneously (Figure 7), with much less error (SSD = 4.58) compared to the same model with constant parameters (SSD = 7.68). Therefore we suggest using simple, zonal models, such as that for a discrete composite media or a facies model, for cases where the subsurface heterogeneity is strong and the heterogeneity information is limited.

[43] The larger scale index [$\alpha = 1.6$, compared to that of the FF-ADE and FD-ADE ($\alpha = 1.1$)] of the calibrated FFD-ADE (15) is mainly due to the fact that the leading edge is mostly produced by fractional advection in the FFD-ADE, while it is mainly caused by fractional dispersion in the FF/FD-ADE. The leading tail of the MADE-2 data resembles a power law of order $x^{-1.5} \sim -1.7$ (Figure 8), which leads to an estimate $\alpha \approx 1.6$ for the FFD-ADE (15) with constant transport parameters (see also the study by *Baeumer et al.* [2001] for a similar model and conclusion). The transport in the MADE site is probably advection-dominated [*Lu et al.*, 2002], and thus the advective travel distance might be larger than the heterogeneity scales, supporting the application of the FFD-ADE (15) (see the discussion in section 2.3). The leading edge might be caused mainly by the advection within high-permeable preferential paths (i.e., ancient channel deposits). We stress that all of the models are linked by the fact that the dispersion process is a result of large "particle" motions [see equations (10), (13), and (17)], whether these are considered differential advection or pure "dispersion," or both.

[44] The scale index $\alpha = 1.1$ used by the FF-ADE (4) and the FD-ADE (11) was a best estimate based on the calculated K statistics (supported by the plume variance growth rate), when the original fADE (1) is used (see the work of *Benson et al.* [2001] for details and *Aban et al.* [2006] for an updated analysis of the K statistics). If the somehow irregular power law slope of the leading edge (Figure 8) is not constant but rather indicates a space-dependent decay
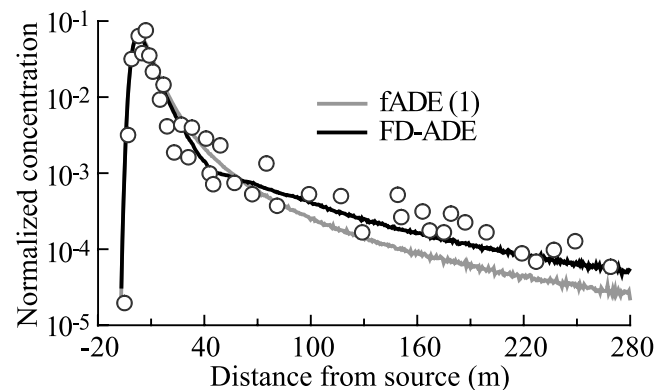

Figure 7. Measured (circles) versus the simulated (lines) resident concentrations using the original fADE (1) with constant parameters, and the FD-ADE (11) with zonal parameters (see the text) for day 224.
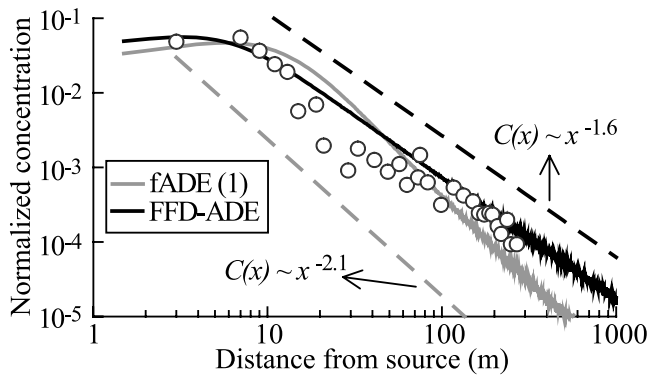
Figure 8. Measured (circles) versus simulated (solid lines) resident concentrations using the original fADE (1) and the FFD-ADE (15) for day 328. Parameters are shown in Table 2.

rate, then the scale index $\alpha = 1.1$ with a space-dependent dispersion coefficient may be used instead of the original fADE (1) with a constant D. The leading tail of the plume captured by the original fADE (1) with scale index α approximates a power law of constant order $x^{-\alpha-1}$, while the leading tail of the plume captured by the FF-ADE (4) or the FD-ADE (11) with scale index α can resemble a power law of order varying with space x. That is why the FF-ADE (4) and the FD-ADE (11) lead to better fits. However, if the power law slope of the leading edge is actually constant (or the leading edge decays with a constant speed), then the FFD-ADE (15) with constant parameters is a better fitting tool.

[45] All three fADE extensions can improve the plume fitting significantly compared to the currently widely used fADE with constant parameters. The FD-ADE model may be more favorable because of (1) its ease of implementation (compared to the two other models), (2) the corresponding (nearly identical) Langevin Markov equation compared to the FF-ADE for linear D, and (3) the consistency with previous analyses of the MADE site K statistics. However, more field applications are needed to check this conclusion. In addition, we emphasize here that the above models of the MADE site are mixtures of prediction and fit. More specifically, for example, the fundamental parameter (α) used in the FD/FF-ADE comes from the K data [*Benson et al.*, 2001] and is not changed. To evaluate the changes that arise from space variability of V and D in all three fADE extensions, we allow those parameters to change to achieve the least error with the data. Results show that the best fit V is within the range of field estimates (predictions) for all models, and thus we conclude that we can use the model that is easiest to implement and/or provides the best fit.

[46] Both the fADEs and the random walk approximations can be extended to more space dimensions and fractal mobile/immobile models. In the mobile/immobile models, the particle trapping time is often assumed to be independent of the subsequent jump length, and thus the stagnant time for each particle trapped by the immobile domain can be "added" directly prior to the motion of the particle. Also, as shown by *Zhang et al.* [2006b], the high-dimensional transport may be characterized by direction-dependent scaling rates and a general mixing measure defining the diffusion strength, which cannot be simulated by the simple model in the work of *Lu et al.* [2002]. A preliminary

modeling of the two-dimensional MADE-2 tritium plume considering mass decay was shown by *Zhang et al.* [2006c], which also indicated the necessity of using a fADE with space-variable transport parameters. Further extension and analysis using the fADEs discussed in this study for fitting the multidimensional and decaying MADE site plumes will be pursued elsewhere.

5. Conclusions

[47] 1. To include the effects of nonstationarity in highly heterogeneous aquifers, the nonlocal fADE with constant parameters may be extended to allow the local variation of spreading strength. Three different fADEs with space-dependent transport parameters, including the FF-ADE, the FD-ADE, and the FFD-ADE, are therefore developed using the generalized mass balance law proposed by *Meerschaert et al.* [2006]. The FF-ADE arises when the classical Fick's law is generalized. The FD-ADE can be derived if the net inflow of dispersive flux uses a fractional divergence. When the total net inflow is a fractional form, the original fADE extends to the FFD-ADE with fully fractional divergence.

[48] 2. Simple Langevin equations can be found in many cases for the three fADE extensions. The Lagrangian stochastic process defined by each Markovian Langevin model describes the microscopic dynamics of each solute particle, and the corresponding particle number density represents the macroscopic (ensemble) average of particle motions. The Lagrangian stochastic process can be conditioned directly on local aquifer properties (i.e., velocity and dispersion coefficient) at any practical, measurable level and resolution, and thus it motivates and supports the application of the spatially nonlocal transport model with local parameters (i.e., the fADE extension) to characterize the solute transport through media with nonstationary heterogeneity.

[49] 3. As shown in Appendix A, the three fADEs discussed in this study cannot be obtained from *Cushman et al.*'s [1994] nonlocal constitutive theory, unless the transport parameters are constant. The dispersive flux with spatially variable parameters is not a space convolution of dispersion coefficient and solute concentration (or its gradient), deviating from those authors' convolutional expression of the nonlocal dispersive flux. Furthermore, if the memory kernels in *Cushman et al.*'s [1994] nonlocal dispersive flux can be extended to contain local information, such as the conditional, nonlocal dispersive flux proposed by *Neuman* [1993], then all three fADEs are special cases of the nonlocal model with the extended memory kernels.

[50] 4. The FF-ADE (4) and the FD-ADE (11) capture identical plume behavior if the dispersion coefficient D varies linearly with distance and $\partial D/\partial x$ is relatively small compared to D. In this case, either equation can be simulated by a random walk using the same Markov process. However, when D is nonlinear and the scale index α is small, the FD-ADE (11) imparts slightly more drift than the FF-ADE (4). In addition, both Lagrangian dynamic analysis and numerical experiments show that the discrepancy between the FFD-ADE and the FD/FF-ADE increases with a decrease of either the fractional dispersivity or the scale index.

[51] 5. To simulate the nuances of the one-dimensional, positively skewed plume with near-source peak and heavy leading tail observed at the MADE site, either the FD-ADE (11) with zonal dispersion coefficients or the FFD-ADE

(15) with constant parameters can be used. The FD-ADE is consistent with previous analysis of the K statistics and might be favored on the basis of a priori estimation of equation parameters.

Appendix A: Relationship Between the fADEs and the Nonlocal Dispersive Constitutive Theories

[52] According to the nonlocal dispersive constitutive theory, the nonlocal total flux for preasymptotic dispersion in one-dimensional space is of the form [*Cushman et al.*, 1994; *Cushman and Ginn*, 2000]

$$
Q(x,t) = \langle V \rangle C + \int_0^t \int_R B_1(y,t,\tau) C(x-y,t-\tau) \mathrm{d}y \mathrm{d}\tau
$$
$$
- \int_0^t \int_R B_2(y,t,\tau) \frac{\partial C(x-y,t-\tau)}{\partial(x-y)} \mathrm{d}y \mathrm{d}\tau, \quad (A1)
$$

where the symbol $\langle \rangle$ denotes the expected value, B_1 and B_2 are the memory kernels, and R denotes the one-dimensional Euclidean space. A more detailed discussion of the above flux is given by *Cushman* [1997, chapter 2]. Under certain constraints [see *Cushman et al.*, 1994], equation (A1) is a convolution on both space and time

$$
Q(x,t) = \langle V \rangle C - \int_0^t \int_R B_2(y,\tau) \frac{\partial C(x-y,t-\tau)}{\partial(x-y)} \mathrm{d}y \mathrm{d}\tau. \quad (A2)
$$

The second term on the RHS of equation (A1) can be neglected when the advective travel distance is small relative to the scales of heterogeneity [*Cushman et al.*, 1994]. This condition is (see equation (57) in the study by *Cushman et al.* [1994])

$$
\int_0^{T_m} \| \langle V(\tau) \rangle \| \, \mathrm{d}\tau \ll L, \quad (A3)
$$

where $V(\tau)$ is the velocity, T_m is the relaxation time of the solute displacement fluctuation, and L is a measure of length of medium uniformity, such as a correlation length. This condition, also called the local equilibrium assumption, denotes a reduction from nonequilibrium displacement fluctuations to equilibrium behavior within the scale of L (see section 7 in the study by *Cushman et al.* [1994] for details).

[53] The advection-dispersion equation with the nonlocal total flux defined by equation (A1) is of the form

$$
\frac{\partial C(x,t)}{\partial t} = -\frac{\partial}{\partial x}[\langle V \rangle C(x,t)] - \frac{\partial}{\partial x} \int_0^t \int_R B_1(y,t,\tau)
$$
$$
\times C(x-y,t-\tau) \mathrm{d}y \mathrm{d}\tau + \frac{\partial}{\partial x} \int_0^t \int_R B_2(y,t,\tau)
$$
$$
\times \frac{\partial C(x-y,t-\tau)}{\partial(x-y)} \mathrm{d}y \mathrm{d}\tau. \quad (A4)
$$

Assuming time locality and using the Fourier transform $(x \to k)$ on equation (A4), we get

$$
\frac{\mathrm{d}}{\mathrm{d}t} \hat{C}(k,t) = -(ik)\langle \hat{V} \rangle(k) \star \hat{C}(k,t) - (ik)\hat{B}_1(k,t) \cdot \hat{C}(k,t)
$$
$$
+ (ik)\hat{B}_2(k,t) \cdot [(ik)\hat{C}(k,t)], \quad (A5)
$$

where the hat denotes the Fourier transform, using the fact that a convolution in real space corresponds to a product in Fourier space (and vice versa), and the symbol $\star$ denotes the convolution.

[54] By choosing a specific kernel B_2 in equation (A4) of the form

$$
B_2(y,\tau) = \frac{D\delta(\tau)H(y)}{\Gamma(2-\alpha)y^{\alpha-1}}, \quad (A6)
$$

and ignoring the second term on the RHS of equation (A4) (or in other words, $B_1 = 0$), *Cushman and Ginn* [2000] found that the original fADE (1) is a special case of the nonlocal ADE (A4). Note that convolution with this kernel is a Riemann-Liouville fractional integral of order $2 - \alpha$, which combines with the two first-order derivatives to produce a fractional derivative of order α. Note also that we assume the far upstream concentration eventually falls to zero, so that the Caputo and Riemann-Liouville forms coincide. In equation (A6), D is a constant, $\delta(\tau)$ is the Dirac delta function and $0 \le \tau \le t$, and $H(y)$ is the Heaviside function on $(0, \infty)$. Physically, as elucidated by *Cushman and Ginn* [2000], this kernel results in a time-local [from $\delta(\tau)$] and upstream space nonlocal [from $H(y)$] dispersive flux with power law decay (from $y^{-(\alpha-1)}$) of the weighted contributions of the neighbors' concentration gradient.

[55] In the following subsections, we explore the relationship between the nonlocal dispersive constitutive theory and the fADEs (4), (11), and (15) by comparing the memory kernels B_1 and B_2 in equation (A4) to the transport parameters in the fADEs. This exploration helps to reveal further the physical meaning that underlies each fADE extension. In particular, the memory kernel can indicate directly how the local (or space-dependent) aquifer information is "remembered" by, or conveyed to the nonlocal dispersion of, solute particles.

A1. The FF-ADE (4)

[56] The FF-ADE (4) has the Fourier transform:

$$
\frac{\mathrm{d}}{\mathrm{d}t} \hat{C}(k,t) = -(ik)\hat{V}(k) \star \hat{C}(k,t) + (ik)\left\{\hat{D}(k) \star \left[(ik)^{\alpha-1}\hat{C}(k,t)\right]\right\}. \quad (A7)
$$

Here the net dispersive flux is a convolution in Fourier space, instead of the product embedded in the dispersive flux shown in equation (A5) (note the net advective flux is a convolution in Fourier space in both cases). Thus the FF-ADE (4) contains a different nonlocality compared to equation (A4), and it is not a special case of equation (A4) unless D is a constant.

[57] To further demonstrate this difference, we expand the dispersive flux $F = -D\partial^{\alpha-1}C/\partial x^{\alpha-1}$ in equation (4) to its integral form

$$
F(x,t) = -D(x)\frac{\partial^{\alpha-1}}{\partial x^{\alpha-1}}C(x,t)
$$
$$
= -D(x)\frac{1}{\Gamma(2-\alpha)}\int_0^\infty \frac{1}{y^{\alpha-1}}\frac{\partial C(x-y,t)}{\partial(x-y)}\mathrm{d}y
$$
$$
= -\int_{-\infty}^\infty \frac{D(x)H(y)}{\Gamma(2-\alpha)y^{\alpha-1}}\frac{\partial C(x-y,t)}{\partial(x-y)}\mathrm{d}y
$$
$$
= -\int_0^t \int_{-\infty}^\infty \frac{D(x)\delta(\tau)H(y)}{\Gamma(2-\alpha)y^{\alpha-1}}\frac{\partial C(x-y,t-\tau)}{\partial(x-y)}\mathrm{d}y\mathrm{d}\tau, \quad (A8)
$$

which is similar to equation (10) in the work of *Cushman and Ginn* [2000] except that D is not limited to be constant here. Hence equation (4) does not reduce to the nonlocal ADE of *Cushman and Ginn* [2000].

[58] *Neuman* [1993] and *Neuman and Orr* [1993] presented a conditional, two-point form, nonlocal dispersive flux, where the memory kernels are conditional estimates with the form $B_1(x, t; y, \tau)$ and $B_2(x, t; y, \tau)$. As discussed by *Neuman* [1993], since this nonlocal constitutive theory deals with conditional estimates rather than their unconditional ensemble mean values, it is less dependent on the ergodicity requirement than the corresponding unconditional theory (such as in the study by *Cushman* [1991]). By selecting

$$B_1(x, t; y, \tau) = 0, \tag{A9a}$$

$$B_2(x, t; y, \tau) = \frac{D(x)\delta(\tau)H(y)}{\Gamma(2-\alpha)y^{\alpha-1}}, \tag{A9b}$$

the FF-ADE (4) is a special case of *Neuman*'s [1993] nonlocal model. Physically, the kernel B_2 defined by equation (A9b) indicates that the influence of any upstream neighbor on the dispersive flux at the current (downstream) position depends on the dispersion strength at the current position. No matter how strong the dispersion coefficient is at any upstream zone, it will not drive more or less solutes downstream. In addition, the kernel B_2 (and actually all B_2 in Appendix A) shows that the contribution of upstream zones increases with a decrease of the space scale index α, corresponding to the fact that a smaller-scale index represents a higher nonlocality.

A2. The FD-ADE (11)

[59] Similarly, we can expand the dispersive flux $F = -\frac{\partial^{\alpha-2}}{\partial x^{\alpha-2}}\left[D\frac{\partial C}{\partial x}\right]$ in the FD-ADE (11) to its integral form

$$
\begin{aligned}
F(x, t) &= -\frac{\partial^{\alpha-2}}{\partial x^{\alpha-2}}\left[D(x)\frac{\partial C}{\partial x}\right] \\
&= -\frac{1}{\Gamma(2-\alpha)}\int_0^\infty \frac{1}{y^{\alpha-1}}\left[D(x-y)\frac{\partial C(x-y, t)}{\partial(x-y)}\right]dy \\
&= -\int_{-\infty}^\infty \frac{D(x-y)H(y)}{\Gamma(2-\alpha)y^{\alpha-1}}\frac{\partial C(x-y, t)}{\partial(x-y)}dy \\
&= -\int_0^t\int_{-\infty}^\infty \frac{D(x-y)\delta(\tau)H(y)}{\Gamma(2-\alpha)y^{\alpha-1}}\frac{\partial C(x-y, t-\tau)}{\partial(x-y)}dyd\tau,
\end{aligned}
\tag{A10}
$$

Again, when D is constant and we select $B_1 = 0$, and B_2 is the same as equation (A6), the FD-ADE (11) is a special case of *Cushman et al.*'s [1994] nonlocal ADE (A4). When D varies in space and we select

$$B_1(x, t; y, \tau) = 0, \tag{A11a}$$

$$B_2(x, t; y, \tau) = \frac{D(x-y)\delta(\tau)H(y)}{\Gamma(2-\alpha)y^{\alpha-1}}, \tag{A11b}$$

the FD-ADE (11) is a special case of *Neuman*'s [1993] nonlocal ADE model. Note also the difference between the kernels B_2: For the FF-ADE, the kernel depends on $D(x)$ at location x, while for the FD-ADE, it depends on $D(x-y)$ at the upstream

location $x-y$. From a particle tracking point of view, this is the difference between taking into account the material properties at the starting point $x-y$ of the jump or the end point x.

A3. The FFD-ADE (15)

[60] For the case where the convective velocity is much larger than the scales of heterogeneity [which violates the local equilibrium assumption (A3)]

$$\int_0^{T_m} \|\langle V(\tau)\rangle\| d\tau \gg L, \tag{A12}$$

then the second term on the RHS of (equation A1) cannot be neglected. Instead, this term is much larger than the flux caused by the average velocity $\langle V \rangle$ and should be accounted in the governing equation.

[61] Similarly, we expand the dispersive flux on the RHS of equation (16) to get

$$
\begin{aligned}
F(x, t) &= \frac{\partial^{\alpha-2}}{\partial x^{\alpha-2}}\left[V(x)C - D(x)\frac{\partial C}{\partial x}\right] \\
&= \int_0^t\int_{-\infty}^\infty \frac{V(x-y)\delta(\tau)H(y)}{\Gamma(2-\alpha)y^{\alpha-1}}C(x-y, t-\tau)dyd\tau \\
&\quad - \int_0^t\int_{-\infty}^\infty \frac{D(x-y)\delta(\tau)H(y)}{\Gamma(2-\alpha)y^{\alpha-1}}\frac{\partial C(x-y, t-\tau)}{\partial(x-y)}dyd\tau.
\end{aligned}
\tag{A13}
$$

Again, when V and D are constant, and we select

$$B_1(y, t, \tau) = \frac{V\delta(\tau)H(y)}{\Gamma(2-\alpha)y^{\alpha-1}}, \tag{A14a}$$

$$B_2(y, t, \tau) = \frac{D\delta(\tau)H(y)}{\Gamma(2-\alpha)y^{\alpha-1}}, \tag{A14b}$$

then the FFD-ADE (15) is a special case of Cushman's nonlocal constitutive theory (A4). If V and D vary in space, and we select

$$B_1(x, t; y, \tau) = \frac{V(x-y)\delta(\tau)H(y)}{\Gamma(2-\alpha)y^{\alpha-1}}, \tag{A15a}$$

$$B_2(x, t; y, \tau) = \frac{D(x-y)\delta(\tau)H(y)}{\Gamma(2-\alpha)y^{\alpha-1}}, \tag{A15b}$$

the FFD-ADE (15) is a special case of *Neuman*'s [1993] nonlocal model. Note here that the local information of both velocity and dispersion coefficient at the starting point is captured by the particle while moving downstream. We emphasize here that the only difference between our fADE extensions and *Neuman*'s [1993] nonlocal theory is that we have specific, power law memory kernels, representing the power law decay of "memory" of local aquifer properties on downstream concentrations.

Appendix B: Derivation of Equation (17)

[62] The Langevin equation for a given space-fractional Fokker-Planck equation (fFPE) with variable coefficients

was derived in the study by *Zhang et al.* [2006a]. The fFPE (forward equation)

$$\frac{\partial P}{\partial t} = \bar{D}p \frac{\partial^\alpha}{\partial x^\alpha}[B(x,t)^\alpha P] + \bar{D}q \frac{\partial^\alpha}{\partial(-x)^\alpha}[B(x,t)^\alpha P] \qquad (B1)$$

with $1 < \alpha < 2$, $B(x,t) \geq 0$, $0 \leq p \leq 1$, $0 \leq q \leq 1$, $p + q = 1$, and $\bar{D} = -1/\cos(\pi\alpha/2) > 0$ corresponds to a Markov process X_t specified in terms of the Langevin equation

$$dX_t = B(x,t)dS_{\alpha,\beta}(t), \qquad (B2)$$

where $S_{\alpha,\beta}(t)$ is a standard stable process in the parameterization of *Samorodnitsky and Taqqu* [1994] (i.e., the scale parameter $\sigma = 1$ and the shift $\mu = 0$) with power law tail index α and arbitrary skewness $\beta = p - q$. The corresponding backward equation is

$$\frac{\partial Q}{\partial t} = \bar{D}pB(x,t)\frac{\partial^\alpha Q}{\partial(-x)^\alpha} + \bar{D}qB(x,t)\frac{\partial^\alpha Q}{\partial x^\alpha}. \qquad (B3)$$

These same relations also hold in the case $0 < \alpha < 1$, except that now the coefficient $\bar{D} = -1/\cos(\pi\alpha/2) < 0$. Additional additive terms in the fFPE correspond to additional additive terms in the backward equation and additional independent additive terms in the corresponding Langevin equation.

[63] Now we apply this method to obtain the Langevin equation (17) for the particle tracking solution of the FFD-ADE (15). Use the product rule to rewrite equation (15) in the form

$$\begin{aligned}\frac{\partial C(x,t)}{\partial t} &= -\frac{\partial^{\alpha-1}}{\partial x^{\alpha-1}}[V(x)C] + \frac{\partial^{\alpha-1}}{\partial x^{\alpha-1}}\left[D(x)\frac{\partial C}{\partial x}\right] \\ &= -\frac{\partial^{\alpha-1}}{\partial x^{\alpha-1}}[V(x)C] + \frac{\partial^\alpha}{\partial x^\alpha}[D(x)C] - \frac{\partial^{\alpha-1}}{\partial x^{\alpha-1}}\left[C\frac{\partial D}{\partial x}\right],\end{aligned}$$
$$(B4)$$

Now a little algebra shows that equation (B4) with $1 < \alpha < 2$, $V(x) \geq 0$, and $D(x) \geq 0$ can be solved by particle tracking via the Langevin equation

$$\begin{aligned}dX_t &= [V(x)\cos(\pi(\alpha-1)/2)]^{\frac{1}{\alpha-1}} \; dS_{\alpha-1,1}(t) \\ &+ [-D(x)\cos(\pi\alpha/2)]^{\frac{1}{\alpha}} dS_{\alpha,1}(t) \\ &+ \Theta[|\partial D/\partial x|\cos(\pi(\alpha-1)/2)]^{\frac{1}{\alpha-1}} \; d\tilde{S}_{\alpha-1,1}(t),\end{aligned} \qquad (B5)$$

where $\Theta = 1$ for $\partial D/\partial x \geq 0$ and $\Theta = -1$ otherwise, and the three standard stable processes $S_{\alpha-1,1}(t)$, $S_{\alpha,1}(t)$, and $\tilde{S}_{\alpha-1,1}(t)$ are all independent with skewness $\beta = 1$. For example, the third term comes from setting $-|\partial D/\partial x| = \bar{D}pB^{\alpha-1}$ with $p = 1$ and solving for B, noting that $\bar{D} < 0$. Observe that the particle jumps described by the fractional advection defined in equation (B5) are always positive, since the index $\alpha - 1$ is between 0 and 1. These jumps represent the fast forward (downstream) movement of solute particles along preferential flow paths. Finally we set

$$\begin{aligned}dL_{\alpha-1}(t) &= \cos(\pi(\alpha-1)/2)^{\frac{1}{\alpha-1}} \; dS_{\alpha-1,1}(t) \\ dL_\alpha(t) &= [-\cos(\pi\alpha/2)]^{\frac{1}{\alpha}} \; dS_{\alpha,1}(t) \\ d\tilde{L}_{\alpha-1}(t) &= \cos(\pi(\alpha-1)/2)^{\frac{1}{\alpha-1}} \; d\tilde{S}_{\alpha-1,l}(t)\end{aligned} \qquad (B6)$$

to arrive at the Langevin equation (17).

References

Aban, I. B., M. M. Meerschaert, and A. K. Panorska (2006), Parameter estimation for the truncated Pareto distribution, *J. Am. Stat. Assoc.*, *101*(473), 270–277.

Adams, E. E., and L. W. Gelhar (1992), Field study of dispersion in a heterogeneous aquifer: 2. Spatial moment analysis, *Water Resour. Res.*, *28*(12), 3293–3307.

Baeumer, B., D. A. Benson, M. M. Meerschaert, and S. W. Wheatcraft (2001), Subordinated advection-dispersion equation for contaminant transport, *Water Resour. Res.*, *37*(6), 1543–1550.

Barlebo, H. C., M. C. Hill, and D. Rosbjerg (2004), Investigating the Macrodispersion Experiment (MADE) site in Columbus, Mississippi, using a three-dimensional inverse flow and transport model, *Water Resour. Res.*, *40*, W04211, doi:10.1029/2002WR001935.

Benson, D. A. (1998), The fractional advection-dispersion equation: Development and application, Ph.D. dissertation, Univ. of Nev., Reno.

Benson, D. A., S. W. Wheatcraft, and M. M. Meerschaert (2000a), Application of a fractional advection-dispersion equation, *Water Resour. Res.*, *36*(6), 1403–1412.

Benson, D. A., S. W. Wheatcraft, and M. M. Meerschaert (2000b), The fractional-order governing equation of Lévy motion, *Water Resour. Res.*, *36*(6), 1413–1423.

Benson, D. A., R. Schumer, M. M. Meerschaert, and S. W. Wheatcraft (2001), Fractional dispersion, Lévy motion, and the MADE tracer tests, *Transp. Porous Media*, *42*(1/2), 211–240.

Berkowitz, B., and H. Scher (1998), Theory of anomalous chemical transport in random fracture network, *Phys. Rev. E*, *57*(5), 5858–5869.

Berkowitz, B., J. Klafter, R. Metzler, and H. Scher (2002), Physical pictures of transport in heterogeneous media: Advection-dispersion, random-walk, and fractional derivative formulations, *Water Resour. Res.*, *38*(10), 1191, doi:10.1029/2001WR001030.

Boggs, J. M., and E. E. Adams (1992), Field study of dispersion in a heterogeneous aquifer: 4. Investigation of adsorption and sampling bias, *Water Resour. Res.*, *28*(12), 3281–3291.

Boggs, J. M., S. C. Young, and L. M. Beard (1992), Field study of dispersion in a heterogeneous aquifer: 1. Overview and site description, *Water Resour. Res.*, *28*(12), 3281–3291.

Bromly, M., and C. Hinz (2004), Non-Fickian transport in homogeneous unsaturated repacked sand, *Water Resour. Res.*, *40*, W07402, doi:10.1029/2003WR002579.

Chang, F. X., J. Chen, and W. Huang (2005), Anomalous diffusion and fractional advection-diffusion equation, *Acta Phys. Sin.*, *54*(3), 1113–1117.

Cushman, J. H. (1991), On diffusion in fractal porous media, *Water Resour. Res.*, *27*(4), 643–644.

Cushman, J. H. (1997), *The Physics of Fluids in Hierarchical Porous Media: Angstroms to Miles*, 467 pp., Springer, New York.

Cushman, J. H., and T. R. Ginn (2000), Fractional advection-dispersion equation: A classical mass balance with convolution-Fickian flux, *Water Resour. Res.*, *36*(12), 3763–3766.

Cushman, J. H., B. X. Hu, and T. R. Ginn (1994), Nonequilibrium statistical mechanics of preasymptotic dispersion, *J. Stat. Phys.*, *75*(5/6), 859–878.

Deng, Z.-Q., V. P. Singh, and L. Bengtsson (2004), Numerical solution of fractional advection-dispersion equation, *J. Hydraul. Eng.*, *130*(5), 422–431.

Deng, Z.-Q., J. de Lima, M. De Lima, and V. P. Singh (2006), A fractional dispersion model for overland solute transport, *Water Resour. Res.*, *42*, W03416, doi:10.1029/2005WR004146.

Dentz, M., and D. M. Tartakovsky (2006), Delay mechanisms of non-Fickian transport in heterogeneous media, *Geophys. Res. Lett.*, *33*, L16406, doi:10.1029/2006GL027054.

Dentz, M., A. Cortis, H. Scher, and B. Berkowitz (2004), Time behavior of solute transport in heterogeneous media: Transition from anomalous to normal transport, *Adv. Water Resour.*, *27*, 155–173.

Eggleston, J., and S. Rojstaczer (1998), Identification of large-scale hydraulic conductivity trends and the influence of trends on contaminant transport, *Water Resour. Res.*, 34(9), 2155–2168.

Feehley, C. E., C. Zheng, and F. J. Molz (2000), A dual-domain mass transfer approach for modeling solute transport in heterogeneous porous media, application to the MADE site, *Water Resour. Res.*, 36(9), 2051–2515.

Feller, W. (1971), *An Introduction to Probability Theory and Its Applications*, v. II, 2nd ed., John Wiley, Hoboken, N. J.

Fogg, G. E. (2004), The hydrofacies approach and why lnK $\sigma < 5–10$ is unlikely, *Eos Trans. AGU*, 85(47), Fall Meet. Suppl., Abstract H13H-01.

Fogg, G. E., S. F. Carle, C. Green (2000), A connected-network paradigm for the alluvial aquifer system. In: D. Zhang (ed.), *Theory, modeling and field investigation in hydrology: A special volume in Honor of Schlomo P. Neuman's 60th Birthday*, Geological Society of America Special Publication, pp. 25–42.

Garabedian, S. P. (1987), Large-scale dispersive transport in aquifers: Field experiments and reactive transport theory, Ph.D. dissertation, Mass. Inst. of Technol., Cambridge.

Grabasnjak, M. (2003), Random particle motion and fractional-order dispersion in highly heterogeneous aquifers, Thesis, Univ. of Nev., Reno.

Harvey, C. F., and S. M. Gorelick (2000), Rate-limited mass transfer or macrodispersion: Which dominates plume evolution at the Macrodispersion Experiment (MADE) site?, *Water Resour. Res.*, 36(3), 637–650.

Herrick, M. G., D. A. Benson, M. M. Meerschaert, and K. R. McCall (2002), Hydraulic conductivity, velocity, and the order of the fractional dispersion derivative in a highly heterogeneous system, *Water Resour. Res.*, 38(11), 1227, doi:10.1029/2001WR000914.

Hill, M. C., H. C. Barlebo, and D. Rosbjerg (2006), Reply to comment by F. Molz et al. on ''Investigating the Macrodispersion Experiment (MADE) site in Columbus, Mississippi, using a three-dimensional inverse flow and transport model'', *Water Resour. Res.*, 42, W06604, doi:10.1029/2005WR004624.

Huang, G. H., Q. Z. Huang, and H. B. Zhan (2006), Evidence of one-dimensional scale-dependent fractional advection-dispersion, *J. Contam. Hydrol.*, 85, 53–71.

Julian, H. E., J. M. Boggs, C. Zheng, and C. E. Feehley (2001), Numerical simulation of a natural gradient tracer experiment for the natural attenuation study: Flow and physical transport, *Ground Water*, 39(4), 534–545.

Killey, R. W. D., and G. L. Moltyaner (1988), Twin Lake tracer test: Setting, methodology, and hydraulic conductivity distribution, *Water Resour. Res.*, 24(1), 1585–1612.

Kim, S., and M. L. Kavvas (2006), Generalized Fick's law and fractional ADE for pollutant transport in a river: Detailed derivation, *J. Hydrol. Eng.*, 11(1), 80–83.

Kohlbecker, M., S. W. Wheatcraft, and M. M. Meerschaert (2006), Heavy tailed log hydraulic conductivity distributions imply heavy tailed log velocity distributions, *Water Resour. Res.*, 42(4), W04411, doi:10.1029/2004WR003815.

LaBolle, E. M., and G. E. Fogg (2001), Role of molecular diffusion in contaminant migration and recovery in an alluvial aquifer system, *Transp. Porous Media*, 42, 155–179.

LaBolle, E. M., and Y. Zhang (2006), Reply to Comment by Doo-Hyun Lim on ''Diffusion processes in composite porous media and their numerical integration by random walks: Generalized stochastic differential equations with discontinuous coefficients'', *Water Resour. Res.*, 42, W02602, doi:10.1029/2005WR004403.

LaBolle, E. M., G. E. Fogg, and A. F. B. Tompson (1996), Random-walk simulation of transport in heterogeneous porous media: Local mass-conservation problem and implementation methods, *Water Resour. Res.*, 32(3), 393–583.

LaBolle, E. M., J. Quastel, and G. E. Fogg (1998), Diffusion theory for transport in porous media: Transition-probability densities of diffusion processes corresponding to advection-dispersion equations, *Water Resour. Res.*, 34(7), 1685–1693.

LeBlanc, D. R., S. P. Garabedian, K. M. Hess, L. W. Gelhar, R. D. Quadri, K. G. Stollenwerk, and W. W. Wood (1991), Large-scale natural gradient tracer test in sand and gravel, Cape Cod, Massachusetts: 1. Experimental design and observed tracer movement, *Water Resour. Res.*, 27(5), 895–910.

Levy, M., and B. Berkowitz (2003), Measurement and analysis of non-Fickian dispersion in heterogeneous porous media, *J. Contam. Hydrol.*, 64, 203–226.

Liu, G., C. Zheng, and S. M. Gorelick (2004), Limits of applicability of the advection-dispersion model in aquifers containing connected high-conductivity channels, *Water Resour. Res.*, 40, W08308, doi:10.1029/2003WR002735.

Lu, S. L., F. J. Molz, and G. J. Fix (2002), Possible problems of scale dependency in applications of the three-dimensional fractional advection-dispersion equation to natural porous media, *Water Resour. Res.*, 38(9), 1165, doi:10.1029/2001WR000624.

Mackay, D. M., D. L. Freyberg, P. V. Roberts, and J. A. Cherry (1986), A natural gradient experiment on solute transport in a sand aquifer: 1. Approach and overview of plume movement, *Water Resour. Res.*, 22(13), 2017–2029.

Meerschaert, M. M., and C. Tadjeran (2004), Finite difference approximations for fractional advection-dispersion flow equations, *J. Comput. Appl. Math.*, 172, 65–77.

Meerschaert, M. M., D. A. Benson, and B. Baeumer (1999), Multidimensional advection and fractional dispersion, *Phys. Rev. E*, 59(5), 5026–5028.

Meerschaert, M. M., D. A. Benson, and B. Baeumer (2001), Operator Lévy motion and multiscaling anomalous diffusion, *Phys. Rev. E*, 63, 021112.

Meerschaert, M. M., J. Mortensen, and S. W. Wheatcraft (2006), Fractional vector calculus, *Physica A*, 367, 181–190.

Miller, K. S., B. Ross (1993), *An Introduction to Fractional Calculus and Fractional Differential Equations*, John Wiley, Hoboken, N. J.

Molz, F. J., C. Zheng, S. M. Gorelick, and C. F. Harvey (2006), Comment on ''Investigating the Macrodispersion Experiment (MADE) site in Columbus, Mississippi, using a three-dimensional inverse flow and transport model'' by Heidi Christiansen Barlebo, Mary C. Hill, and Dan Rosbjerg, *Water Resour. Res.*, 42, W06603, doi:10.1029/2005WR004265.

Neuman, S. P. (1993), Eulerian-Lagrangian theory of transport in space-time nonstationary velocity fields: Exact nonlocal formalism by conditional moments and weak approximation, *Water Resour. Res.*, 29(3), 633–645.

Neuman, S. P., and S. Orr (1993), Prediction of steady state flow in non-uniform geologic media by conditional moments: Exact nonlocal formalism and weak approximation, *Water Resour. Res.*, 29(2), 341–364.

Osler, T. J. (1971), Fractional derivatives and Leibniz rule, *Am. Math. Mon.*, 78(6), 645–649.

Pachepsky, Y., D. Timlin, and D. A. Benson (2001), Transport of water and solutes in soils as in fractal porous media, *Soil Sci. Soc. Am. J.*, 56, 51–75.

Paradisi, P., R. Cesari, F. Mainardi, and F. Tampieri (2001), The fractional Fick's law for non-local transport processes, *Physica A*, 293, 130–142.

Rehfeldt, K. R., J. M. Boggs, and L. W. Gelhar (1992), Field study of dispersion in a heterogeneous aquifer: 3. Geostatistical analysis of hydraulic conductivity, *Water Resour. Res.*, 28(12), 3309–3324.

Samorodnitsky, G., M. S. Taqqu (1994), *Stable Non-Gaussian Random Processes: Stochastic Models With Infinite Variance*, CRC Press, Boca Raton, Fla.

Schumer, R., D. A. Benson, M. M. Meerschaert, and S. W. Wheatcraft (2001), Eulerian derivation of the fractional advection-dispersion equation, *J. Contam. Hydrol.*, 38, 69–88.

Schumer, R., D. A. Benson, M. M. Meerschaert, and B. Baeumer (2003a), Multiscaling fractional advection-dispersion equations and their solutions, *Water Resour. Res.*, 39(1), 1022, doi:10.1029/2001WR001229.

Schumer, R., D. A. Benson, M. M. Meerschaert, and B. Baeumer (2003b), Fractal mobile/immobile solute transport, *Water Resour. Res.*, 39(10), 1296, doi:10.1029/2003WR002141.

Trefry, M. G., F. P. Ruan, and D. McLaughlin (2003), Numerical simulations of preasymptotic transport in heterogeneous porous media: Departure from the Gaussian limit, *Water Resour. Res.*, 39(3), 1063, doi:10.1029/2001WR001101.

Tsallis, C., and E. K. Lenzi (2002), Anomalous diffusion: Nonlinear fractional Fokker-Plancker equation, *Chem. Phys.*, 284, 341–347.

Zhang, X. X., J. W. Crawford, L. K. Deeks, M. I. Sutter, A. G. Bengough, and I. M. Young (2005), A mass balance based numerical method for the fractional advection-dispersion equation: Theory and application, *Water Resour. Res.*, 41, W07029, doi:10.1029/2004WR003818.

Zhang, Y., D. A. Benson, M. M. Meerschaert, and H. P. Scheffler (2006a), On using random walks to solve the space-fractional advection-dispersion equations, *J. Stat. Phys.*, 123(1), 89–110.

Zhang, Y., D. A. Benson, M. M. Meerschaert, E. M. LaBolle, and H. P. Scheffler (2006b), Random walk approximation of fractional-order multiscaling anomalous diffusion, *Phys. Rev. E*, 74, 0267062006.

Zhang, Y., D. A. Benson, M. M. Meerschaert, E. M. LaBolle, and H. P. Scheffler (2006c), Lagrangian characterization of contaminant transport through multidimensional heterogeneous media with limited heterogeneity information, *Proceedings of Modflow and More 2006: Managing Ground-Water Systems*, E. Poeter, M. Hill, and C. Zheng (eds.), vol. 2, pp. 639–643.

Zheng, C., and S. M. Gorelick (2003), Analysis of the effect of decimeter-scale preferential flow paths on solute transport, *Ground Water*, *41*(2), 142–155.

Zheng, C., and J. J. Jiao (1998), Numerical simulation of tracer tests in a heterogeneous aquifer, *J. Environ. Eng.*, *124*(6), 510–516.

Zhou, L., and H. M. Selim (2003), Application of the fractional advection-dispersion equation in porous media, *Soil Sci. Soc. Am. J.*, *67*, 1079–1084.

Zinn, B., and C. F. Harvey (2003), When good statistical models of aquifer heterogeneity go bad: A comparison of flow, dispersion, and mass transfer in connected, and multivariate Gaussian hydraulic conductivity fields, *Water Resour. Res.*, *39*(3), 1051, doi:10.1029/2001WR001146.

———————————————

D. A. Benson and Y. Zhang, Department of Geology and Geological Engineering, Colorado School of Mines, Golden, CO 80401, USA. (dbenson@mines.edu; yzhang@mines.edu)

E. M. LaBolle, Hydrologic Sciences, University of California, Davis, CA 95616, USA. (emlabolle@ucdavis.edu)

M. M. Meerschaert, Department of Statistics and Probability, Michigan State University, East Lansing, MI 48824, USA. (mcubed@stt.msu.edu)